

Specific Features of Heavy Quark Production. LPHD approach to heavy particle spectra

Yu.L. Dokshitzer ¹

Theoretical Physics Division, CERN,
CH-1211, Geneva 23, Switzerland,

V.A. Khoze ¹

Centre for Particle Theory, University of Durham,
Durham DH1 3LE, UK,

S.I. Troyan

Institute for Nuclear Physics,
St. Petersburg, Gatchina 188350, Russia

Abstract

Perturbative QCD formula for inclusive energy spectra of heavy quarks from heavy quark initiated jets which takes into account collinear and/or soft logarithms in all orders, the exact first order result and two-loop effects is applied to distributions of heavy flavoured hadrons in the framework of the LPHD concept.

¹on leave of absence from the Institute for Nuclear Physics, St. Petersburg, Gatchina 188350, Russia

1 Introduction

Heavy flavour physics is now extensively studied experimentally at both e^+e^- and hadronic colliders. Experiments at Z^0 have led to the availability of new data on the profiles of jets initiated by heavy quarks [1,2]. Further progress is expected from the measurements at LEP 2 and, especially, at a future linear e^+e^- collider. The principal physics issues of these studies are related not only to testing the fundamental aspects of QCD, but also to their large potential importance for measurements of heavy particle properties: lifetimes, spatial oscillations of flavour, searching for CP-violating effects in their decays *etc.* Properties of b-initiated jets are of primary importance for analysis of the final state structure in $t\bar{t}$ production processes. A detailed knowledge of the b-jet profile is also essential for the Higgs search strategy.

The physics of heavy quarks has always been considered as one of the best testing grounds for QCD. Despite this, not many attempts to derive self-consistent perturbative (PT) results for the profiles of heavy quark jets have appeared so far. This paper is aimed at a condensed presentation of the part of the results of the long-term Leningrad/St.Petersburg QCD group project¹ that concerns PT analysis of the inclusive energy spectra of heavy quarks.

The selection of this subject is motivated by the following topical questions:

- i) To what extent can heavy quark distribution be treated as a purely perturbative (Infrared Safe) quantity?
- ii) Can we describe the gross features of jets initiated by heavy quarks without invoking phenomenological fragmentation schemes?
- iii) What kind of information can be extracted from the measurements of heavy quark energy spectra and, in particular, from the scaling violation effects?

There are two ingredients of the standard Renormalization Group (RG) approach to the description of the energy spectra of heavy flavoured hadrons H_Q . Here one starts from a phenomenological fragmentation function for the

$$Q(x) \rightarrow H_Q(x_H) \quad (1.1)$$

transition and then traces its evolution with the annihilation energy W by means of PT QCD. Realistic fragmentation functions [9] exhibit a parton-model-motivated maximum at (hereafter M is the heavy quark mass)

$$1 - \frac{x_H}{x} \sim \frac{\text{const}}{M}.$$

Taking gluon radiation at the PT-stage of evolution into account would then induce scaling violations that soften the hadron spectrum by broadening (and damping) the original maximum and shifting its position to larger values of $1-x_H$ with W increasing.

This approach has been successfully tried by B. Mele and P. Nason [10], who have studied the effects of multiple soft gluon radiation and have been looking for realistic fragmentation functions to describe the present day situation with heavy particle spectra, and to make reliable

¹for some basic references see [3–8]

predictions for the future. Being formally well justified, such an approach, however, basically disregards the effects that the finite quark mass produces on the accompanying QCD bremsstrahlung pattern, since the W -evolution by itself is insensitive to M (save the power suppressed M^2/W^2 corrections).

At the same time, as far as one may consider M a sufficiently large momentum scale, it is tempting to carry out a program of deriving the predictions that would keep under PT control, as much as possible, the dependence of H_Q distributions on the quark mass.

In Section 2 we present and discuss the PT formula for inclusive quark spectra, $D(x; W, M)$, that in the QED case would give an unambiguous all-order-improved *absolute* prediction for the inclusive energy distribution of muons produced in

$$e^+e^- \rightarrow \mu^\pm(x) \mu^\mp + \dots \quad (1.2)$$

Given an explicit dependence on m_μ , one may theoretically compare, say, the μ and τ spectra, a goal that, generally speaking, can not be achieved within the standard “evolutionary” framework.

In Section 3 the topical questions listed above are addressed. We discuss the problem of “infrared instability” of the PT quark spectra and suggest a solution of this formal difficulty based upon the notion of an “infrared regular” effective coupling. Having regularized the PT expression in this way we observe that the gluon bremsstrahlung effects (Sudakov suppression of the quasi-elastic kinematics $x \rightarrow 1$) lead to particle spectra that have a similar shape to the non-PT fragmentation function.

An emphasis of the rôle of PT dynamics has been successfully tested in studies of light hadron distributions in QCD jets. Prompted by the success of the MLLA-LPHD approach [12], we consider an option of describing the gross features of heavy quark initiated jets entirely by means of PT QCD, without invoking any fragmentation hypothesis.

The LPHD philosophy would encourage us to continue the PT description of an inclusive quantity down to small momentum scales, and with the hope that such an extrapolation of the quark-gluon language would be dual to the sum over all possible hadronic excitations. For the problem under consideration, such an approach could describe the energy fraction distribution averaged over heavy-flavoured hadron states, the mixture that naturally appears, *e.g.*, in the study of inclusive hard leptons.

In Section 4, we report results on the comparison of the PT predictions with the measured c and b energy losses at different annihilation energies. Fitting the rate of scaling violation in $\langle x \rangle(W)$ results in the QCD scale parameter Λ that, after being translated into the popular $\overline{\text{MS}}$ scheme, agrees with the values extracted from other studies. On the other hand, the *absolute* values of $\langle x_{c,b} \rangle$ at a given energy are most sensitive to the behaviour of the radiation intensity, say, below 1–2GeV.

Limited experimental information does not at present allow us to disentangle various possible shapes of α_s^{eff} near the origin. At the same time, a quite substantial difference between $\langle x_c \rangle$ and $\langle x_b \rangle$ fits nicely into PT-controlled mass dependence, provided the characteristic integral of the effective coupling over the “confinement” region assumes a fixed value,

$$\int_0^{2\text{GeV}} dk \frac{\alpha_s^{\text{eff}}(k)}{\pi} \approx 0.38\text{GeV}$$

(with k the linear momentum variable). Given this value, one may predict the differential c and b energy distributions at arbitrary W , predictions which prove to be unaffected in practice by our ignorance of the detailed behaviour of α_s^{eff} in the small momentum region.

In Section 5 the results of the study are discussed and conclusions drawn.

Detailed derivation of the master formula for the inclusive heavy quark energy spectrum is given in Appendices. In Appendix A the problem of running coupling in the perturbative radiator is dealt with. Appendix B is devoted to the second loop effects in the anomalous dimension.

2 Perturbative Energy Spectrum of Leading Quarks

We denote the cms annihilation energy by W , and $M \equiv m \cdot W$ is the quark mass.

Here we describe perturbative QCD result for the inclusive energy spectrum of heavy quarks, $D(x; W, M)$, $x \equiv 2E_Q/W$, produced in $e^+e^- \rightarrow Q(x) + \bar{Q} + \text{light partons}$.

This function has the following properties:

- it embodies the exact first order result ^[13] $D^{(1)} = \alpha_s \cdot f(x; m)$ and, as a consequence,
- it has the correct threshold behaviour at $1 - 2m \ll 1$;
- in the relativistic limit $m \ll 1$, it accounts for all significant logarithmically enhanced contributions in high orders, including
 1. running coupling effects,
 2. the two-loop anomalous dimension and
 3. the proper coefficient function with exponentiated Sudakov-type logs, which are essential in the quasi-elastic kinematics, $(1-x) \ll 1$;
- it takes into full account the controllable dependence on the heavy quark mass that makes possible a comparison between the spectra of b and (directly produced) c quarks.

By “threshold behaviour” we mean here the kinematical region of non-relativistic quarks, $|W - 2M| \sim M$, in which gluon bremsstrahlung acquires additional dipole suppression. At the same time we will not account for the Coulomb effects that would essentially modify the production cross section near the actual threshold, $W - 2M \ll M$ ^[14].

We are mainly interested in the “leading” energy region of x of the order of (or close to) unity. For this reason we disregard in what follows potentially copious production of $Q\bar{Q}$ pairs via secondary gluon splitting², *i.e.* singlet sea contribution, as well as the specific $Q \rightarrow Q + Q\bar{Q}$ transition that appears in the *non-singlet* anomalous dimension beyond the first loop (for a review see [15] and references therein).

Therefore the quark distribution we define below will satisfy the sum rule

$$\int_{2m}^1 dx D(x; W, M) = 1. \quad (2.1)$$

²apart from the integral effect of the unregistered pairs embodied into the running coupling, see below

The accuracy of the PT prediction described in this paper is

$$D(x; W, M) \cdot [1 + \mathcal{O}(\alpha_s^2)] . \quad (2.2)$$

This expansion is *uniform* in x , that is, the α_s^2 correction does not blow up (neither as a power, nor logarithmically) when $(1-x) \rightarrow 0$.

2.1 Definition of the leading quark distribution.

The inclusive cross section for single particle production in e^+e^- annihilation is conveniently written in terms of structure functions as, *e.g.*, ^[15]

$$\sigma_0^{-1} \frac{d\sigma}{dx} = 3\mathcal{F}_L^+(x) + \mathcal{F}_2^+(x) = \mathcal{F}_L^+(x) + \mathcal{F}_T^+(x) , \quad (2.3)$$

with σ_0 the standard Born cross section factor.

We define the normalized inclusive energy spectrum as

$$D(x; W, M) = \sigma_{\text{tot}}^{-1} \frac{d\sigma}{dx} \equiv \int_{\Gamma} \frac{dj}{2\pi i} x^{-j} D_j(W, M) ; \quad (2.4)$$

where the contour Γ runs parallel to the imaginary axis in the complex moment j plane.

Aiming at an *exact* account of the first order QCD effects, we include in σ_{tot} the first α_s correction to the annihilation cross section, that in the case of relativistic quarks reads

$$\sigma_{\text{tot}} = \sigma_0 \left[1 + \frac{3}{2} C_F a + \mathcal{O}(a^2) \right] ; \quad a = a(W^2) \equiv \frac{\alpha_s(W)}{2\pi} , \quad C_F = \frac{N_c^2 - 1}{2N_c} = \frac{4}{3} .$$

With this definition, the structure functions \mathcal{F} in the moment representation become

$$\begin{aligned} \mathcal{F}_\alpha(j) &= c_\alpha(j) \left(1 - \frac{3}{2} C_F a [j^{-1} - 1] \right) D_j \cdot [1 + \mathcal{O}(a^2)] , \\ c_L(j) &= C_F a j^{-1} , \quad c_T(j) = 1 + \frac{1}{2} C_F a j^{-1} , \quad c_2(j) = 1 - \frac{3}{2} C_F a j^{-1} . \end{aligned} \quad (2.5)$$

2.2 The radiator.

The integrand of (2.4) may be written in the exponential form as

$$\ln D_j = \int_{2m}^1 dx [x^{j-1} - 1] \frac{dw(x; W, M)}{dx} , \quad (2.6)$$

where the ‘‘radiator’’ dw/dx originates from the improved first order gluon emission probability, in which finite mass and running coupling effects have been included³. The corresponding expression reads

$$C_F^{-1} v \frac{dw}{dx} = \int_{\kappa^2}^{\mathcal{Q}^2} \frac{dt}{t} \left\{ a(t) \left[\frac{2(x-2m^2)}{1-x} + \zeta^{-1}(1-x) \right] - a'(t)(1-x) + a^2(t)\Delta^{(2)}(x) \right\} \quad (2.7a)$$

$$+ \beta(x) \left\{ -\frac{2x}{1-x} [a(\mathcal{Q}^2) + a(\kappa^2)] + \zeta^{-1} \frac{x(x-2m^2)}{2(1-x)} \left(\frac{1-x}{1-x+m^2} \right)^2 a(\mathcal{Q}^2) \right\} . \quad (2.7b)$$

³Detailed derivation of the radiator is presented in Appendix A; see also [7]

Here the two characteristic momentum scales have been introduced,

$$\begin{aligned}\mathcal{Q}^2 &\equiv \mathcal{Q}^2(x) = W^2 \cdot \frac{(1-x)^2}{1-x+m^2} z_0, \\ \kappa^2 &\equiv \kappa^2(x) = M^2 \cdot \frac{(1-x)^2}{z_0},\end{aligned}\tag{2.8}$$

with

$$z_0 \equiv \frac{1}{2} \left(x - 2m^2 + \sqrt{x^2 - 4m^2} \right) = x + \mathcal{O}(m^2).$$

The following notations were also used:

$$\begin{aligned}m &\equiv \frac{M}{W} \leq \frac{1}{2}; \quad v \equiv \sqrt{1-4m^2}; \quad \beta(x) \equiv \sqrt{1-4m^2/x^2}, \quad 0 \leq \beta \leq v; \quad \zeta = 1+2m^2; \\ a'(k^2) &= \frac{d}{d \ln k^2} a(k^2); \quad a(k^2) \equiv \frac{\alpha_s(k)}{2\pi}.\end{aligned}\tag{2.9}$$

The radiator (2.7) vanishes at

$$x = x_{min} \equiv 2m; \quad \left(\beta(x_{min}) = 0, \quad \mathcal{Q}^2 = WM \frac{(1-2m)^2}{1-m} = \kappa^2 \right),$$

thus justifying the lower kinematical limit in eq.(2.6).

Relativistic Approximation. In the relativistic approximation, $m \ll 1$, we set $v = \beta = \zeta = 1$ to get a simplified expression

$$\begin{aligned}C_F^{-1} \frac{dw}{dx} &= \int_{\kappa^2}^{\mathcal{Q}^2} \frac{dt}{t} \left\{ a(t)P(x) - a'(t)(1-x) + a^2(t)\Delta^{(2)}(x) \right\} \\ &+ a(\mathcal{Q}^2) \left\{ \frac{-2x}{1-x} + \frac{x^2}{2(1-x)} \right\} + a(\kappa^2) \left\{ \frac{-2x}{1-x} \right\};\end{aligned}\tag{2.10a}$$

$$\mathcal{Q}^2 = W^2 x (1-x), \quad \kappa^2 = M^2 (1-x)^2 / x,\tag{2.10b}$$

where

$$P(x) = \frac{1+x^2}{1-x}.\tag{2.11}$$

The integration variable t determines the physical hardness scale of the running coupling, and is related to the transverse momentum of the radiation⁴. In the dominant integration region,

$$k_\perp^2 \ll W^2, \quad t = x \cdot k_\perp^2.\tag{2.12}$$

The lower limit $t \geq \kappa^2$ sets the boundary for the essential gluon emission angles,

$$t \sim E_Q \frac{2}{W} \cdot (\omega_g \Theta)^2 \geq \kappa^2 \sim M^2 \frac{\omega_g^2}{E_Q} \frac{2}{W} \implies \Theta \geq M/E_Q \equiv \Theta_0.$$

This restriction manifests the ‘‘dead cone’’ phenomenon characteristic for bremsstrahlung off a massive particle. It is largely responsible for the differences between radiative particle production in jets produced by a light and a heavy quark (excluding the decay products of the latter), see [4–6].

⁴For the space-like evolution similar relation holds [16] with x^{-1} substituted for x in (2.12)

2.3 Logs and their exponentiation.

Singularities of the radiator (2.7) at $x = 1$, when driven through the inverse Mellin transform (2.4), (2.6), give rise to $\ln(1-x)$ terms. Bearing this in mind, one may represent the term-by-term structure of the radiator by the following symbolic expression,

$$(2.7a) \implies a(CS + S^2) + aC + a^2C + \left[a^2C + \underline{a^2(CS + S^2)} \right]; \quad (2.13a)$$

$$(2.7b) \implies aS + aS + aS, \quad (2.13b)$$

where $C = \ln W/M$ and $S = \ln 1/(1-x)$ represent large logs that usually reflect enhancements due to quasi-collinear and soft gluon radiation respectively. As we shall see shortly, under the “physical” definition of the QCD coupling the last 2nd order term in (2.13a) is free from the double-log contribution (the underlined piece) so that the “convergence” of the PT expansion (2.13) is improved.

Exponentiation of collinear logs follows from the general factorization theorem⁵. Arguments in favour of exponentiation of $aS^2 + aS$ contributions according to (2.6) have been given in [7], motivated by the factorization property of soft bremsstrahlung. Exponentiation of non-logarithmic $\mathcal{O}(a)$ corrections, corresponding to the terms in the non-integral part of the radiator (2.7b) that are *regular* at $(1-x) \rightarrow 0$, is questionable (indeed wrong) and unnecessary within the accuracy adopted (see (2.2)). Keeping such terms in the exponent is a matter of choice. We do so just to simplify the result and make the normalization sum rule (2.1) automatically satisfied, $D_{j=1} \equiv 1$.

When translated into the standard language of the RG motivated approach, the integral part of the radiator (2.10) may be said to embody the anomalous dimension together with (a part of) the correction to the hard cross section due to the x -dependent factor in the upper integration limit:

$$\int^{W^2 x(1-x)} \frac{dt}{t} a(t) P(x) \approx \int^{W^2} \frac{dt}{t} a(t) P(x) + a(W^2) P(x) \ln[x(1-x)] + \mathcal{O}\left(\frac{a^2 \ln^2(1-x)}{1-x}\right). \quad (2.14)$$

Non-uniformity of such an expansion with respect to the potentially large logarithm, $\ln(1-x)$, explains why we preserve the exact kinematical limits in (2.7). By neglecting the last term in (2.14), one would lose control of the $a^2 S^3$ terms. Such contributions formally belong to the 2nd order correction to the hard cross section, and therefore lie beyond the reach of the two-loop RG analysis. In the meantime, such an ignorance would undermine the possibility of keeping track of essential first subleading corrections, $a^n \log^{2n-1}$, at the level of running coupling effects in the quark form factor (Sudakov suppression).

Let us stress that eqs.(2.6), (2.7) solve the problem of all-order resummation of soft radiation effects both in the *hard cross section*⁶ and in the *coefficient function*, that is at low momentum scales $\kappa^2 \propto M^2$. In particular, the term in (2.7b) proportional to $a(\kappa^2)$ (which is W -independent and therefore gets lost in the standard evolution approach) accounts for the *exponentiated* contribution from soft gluons at small emission angles $\Theta < \Theta_0$, $k_\perp^2 \ll M^2$ — the dead cone subtraction

⁵this applies to C -contaminated terms of (2.13a) as well as to the last contribution in (2.13b), that actually is due to *hard* gluons *collinear* to the \bar{Q} momentum (the “backward jet” correction [7])

⁶for a review of such resummation programs see, *e.g.*, [17] and references therein

effect. Notice that the similar term proportional to $a(\mathcal{Q}^2)$ (which does belong to the hard cross section corrections) is due to the dead cone subtraction in the backward jet.

2.4 Second loop effects.

The preliminary result of [7] is improved by taking into full account effects of the two-loop anomalous dimension embodied in the a' and $\Delta^{(2)}$ of (2.7a). We prefer to treat these two terms separately, as the former naturally emerges in the dispersion relation approach to definition of the running coupling [18]. It shows that beyond the first loop the “soft” and the “hard” parts of the GLAP splitting function (2.11) in the anomalous dimension actually acquire different physical interaction strength [16],

$$\gamma^{(1)} = a \cdot \frac{1+x^2}{1-x} \implies \gamma^{(2)} = a \cdot \frac{2x}{1-x} + [a - a'] \cdot (1-x).$$

The actual expression for Δ depends on the renormalization scheme chosen for the one-loop coupling. It may be fixed, *e.g.*, by matching with the known two-loop $\overline{\text{MS}}$ result for the non-singlet fragmentation function. To this end one has to consider the W -dependent part of the relativistic radiator (2.10),

$$\begin{aligned} C_F^{-1} \frac{dw}{dx} &= \int^{W^2 x(1-x)} \frac{dt}{t} \left\{ a_{\overline{\text{MS}}}(t) P(x) - a'(t) (1-x) + a^2(t) \Delta_{\overline{\text{MS}}}^{(2)}(x) \right\} \\ &+ a(W^2) \left\{ \frac{-2x}{1-x} + \frac{x^2}{2(1-x)} \right\} + \text{const} + \mathcal{O}(a^2(W^2)), \end{aligned} \quad (2.15)$$

and, with account of (2.5) relating D to the structure functions, compare the scaling violation rate according to (2.6), (2.15) with that computed in [19–21].

By doing so (see Appendix B) one arrives at ($C_A = N_c = 3$, $T_R = \frac{1}{2}$)

$$\Delta_{\overline{\text{MS}}}^{(2)}(x) = P(x) \cdot \mathcal{K} + \tilde{\Delta}^{(2)}(x); \quad (2.16a)$$

$$\mathcal{K} = \left[C_A \left(\frac{67}{18} - \frac{\pi^2}{6} \right) - \frac{10}{9} n_f T_R \right] = \begin{cases} 4.565 & (n_f = 3), \\ 4.010 & (n_f = 4), \\ 3.454 & (n_f = 5); \end{cases} \quad (2.16b)$$

$$\tilde{\Delta}^{(2)}(x) = C_F \mathcal{V}(x) + \mathcal{R}(x). \quad (2.16c)$$

\mathcal{V} term is responsible for the difference between the time-like and space-like anomalous dimensions. Explicit expressions for $\mathcal{V}(x)$ and $\mathcal{R}(x)$ are given in Appendix B.

Introducing the Physical Coupling. In the $x \rightarrow 1$ limit, $\Delta_{\overline{\text{MS}}}^{(2)}$ (2.16) peaks together with $P(x) \propto (1-x)^{-1}$. At the same time, $\tilde{\Delta}^{(2)}$ is less singular in this limit,

$$\begin{aligned} \mathcal{V}(x)/\Delta^{(2)}(x) &\propto (1-x) \ln(1-x), \\ \mathcal{R}(x)/\Delta^{(2)}(x) &\propto (1-x)^2. \end{aligned}$$

As far as large quark energies are concerned, $\ln 1/(1-x) > 1$, the $\tilde{\Delta}^{(2)}$ term constitutes a small correction. Thus, the major part of the two-loop effect according to (2.16) reduces to a finite renormalization of the leading term $aP(x)$. This naturally suggests absorbing the correction by introducing the “physical” effective coupling according to

$$a_{\overline{\text{MS}}} P(x) + a^2 \Delta_{\overline{\text{MS}}}^{(2)}(x) = a_{\text{eff}} P(x) + a^2 \tilde{\Delta}^{(2)}(x) + \mathcal{O}(a^3); \quad (2.17a)$$

$$a_{\text{eff}} = a_{\overline{\text{MS}}} (1 + a \mathcal{K}), \quad a_{\overline{\text{MS}}} \approx a_{\text{eff}} (1 - a_{\text{eff}} \mathcal{K}). \quad (2.17b)$$

Eq.(2.17b) relates the scale parameters Λ of the two schemes. This relation within two-loop accuracy reads

$$\begin{aligned} \ln \Lambda_{\text{eff}} &= \ln \Lambda_{\overline{\text{MS}}} + \frac{\mathcal{K}}{\beta} = \ln \Lambda_{\overline{\text{MS}}} + \frac{\left(\frac{67}{18} - \frac{\pi^2}{6}\right) C_A - \frac{10}{9} n_f T_R}{\frac{11}{3} C_A - \frac{4}{3} n_f T_R}; \\ \Lambda_{\text{eff}} &= \Lambda_{\overline{\text{MS}}} \times \begin{cases} 1.66 & (n_f = 3), \\ 1.57 & (n_f = 5). \end{cases} \end{aligned} \quad (2.18)$$

Our Λ_{eff} coincides with the Λ_{MC} introduced by Catani, Marchesini and Webber in [22].

Quark Thresholds in the Running Coupling. One additional comment is in order concerning the essence of α_s^{eff} . In spite of the formal equivalence of the two representations (2.17a), the former one is physically preferable since $\tilde{\Delta}^{(2)}(x)$ is free from an ill-defined quantity n_f representing the number of “active” quark flavours. The t -integration in (2.7) runs over a broad region that is sliced by the finite quark mass scales. Naturally, one has to increment n_f when passing such a scale, *e.g.* $n_f = 3 \rightarrow n_f = 4$ when going through $t \approx 1.5 \text{ GeV}$. $\Lambda_{\overline{\text{MS}}}$ has to be redefined by adjusting to a new β -function value, and $\Delta_{\overline{\text{MS}}}$ should be changed accordingly. The problem appears to be entirely technical, however, and reflects a deficiency of the $\overline{\text{MS}}$ prescription as one of the schemes based upon the dimensional regularization technique that eventually treats fermions as massless particles: The discontinuous behaviour of Λ and Δ gets compensated in the physical combination (2.17a) that emerges in the full two-loop anomalous dimension. It is worthwhile to notice that our convention (n_f independent $\tilde{\Delta}^{(2)}(x)$, the scale parameter Λ defined by (2.18)) is in accord with the BLM prescription [23] for optimizing the choice of “physical coupling”.

For the argument sake, one may once again invoke the QED example (1.2). In this context, an application of the $\overline{\text{MS}}$ scheme would reveal the same problem with the lepton thresholds (e, μ, τ etc.), while a_{eff} would be nothing but the *physical* running QED coupling, the one given by the Euclidean photon renormalization function $Z_3(t)$ that is unambiguously linked by the dispersion relation to fermion pair production (with the finite fermion mass effects fully included).

The improved one-loop expression for a_{eff} accounting for finite quark mass effects reads (for a detailed discussion see [16])

$$a_{\text{eff}}^{-1}(Q^2) = \beta_\ell \ln \frac{Q}{\mu} - \frac{2T_R}{3} \sum_i \Pi \left(1 + \frac{4M_i^2}{Q^2} \right) + a_{\text{eff}}^{-1}(\mu^2), \quad (\mu \ll M_i); \quad (2.19a)$$

$$\Pi \approx \begin{cases} \ln(Q^2/M_i^2) - \frac{5}{3}, & Q \gg M_i; \\ 2Q^2/5M_i^2, & Q \ll M_i, \end{cases} \quad (2.19b)$$

where β_ℓ accounts for gluon and massless quark contributions ($\beta_\ell = b_{[n_f=3]} = 9$) and Π is the standard fermion loop polarization operator known from the mid-fifties (see below eq.(3.24)). According to (2.19b), heavy flavours *decouple* at low momentum scales (as they ought to). In the “ultraviolet” regime, Π acquires a constant subtraction from the leading log behaviour, which term, if treated as the two-loop correction, explains the n_f dependent piece of the \mathcal{K} factor (2.16b) that enters the relation (2.17b) between the physical and the $\overline{\text{MS}}$ couplings: $-\frac{10}{9}T_R = \frac{4}{3}T_R \cdot (-\frac{5}{6})$.

$\tilde{\Delta}^{(2)}$ is Practically Negligible. As an estimate of the magnitude of the $\tilde{\Delta}^{(2)}$ correction we present its contribution to the second moment $j=2$ that describes quark energy losses:

$$\begin{aligned} C_F \left\{ a_{\overline{\text{MS}}} P_j (1 + a \mathcal{K}) + a^2 \tilde{\Delta}_j^{(2)} \right\} &= C_F P_j \left\{ a_{\text{eff}} + a^2 \delta_j \right\} + \mathcal{O}(a^3); \\ \delta_2 &= \left[\frac{21}{36} + \left(\frac{85}{36} - \frac{\pi^2}{3} \right) \right] C_F + \frac{31}{36} (C_A - 2C_F) = -0.1735. \end{aligned} \quad (2.20)$$

Being numerically very small already for $j=2$, the relative correction δ_j continues to fall as j^{-1} with j increasing. Therefore in practice one may use (2.7) with $\Delta^{(2)} \equiv 0$, provided the physical effective coupling (2.17b) is used.

2.5 Axial vs. Vector currents in $Q\overline{Q}$ production.

The master equation (2.7) has been written for the case of $Q\overline{Q}$ production via the vector current, in which case

$$\zeta = \zeta_V \equiv \frac{\sigma_{[V]}(v)}{\sigma_{[V]}(1)} = 1 + 2m^2 = \frac{1}{2}(3 - v^2).$$

This factor tends to 1 in the relativistic limit $m \rightarrow 0$ but depends otherwise on the production channel (see Appendix A for details). It is worthwhile to note that beyond the leading twist approximation, generally speaking, there is no way to define the universal *fragmentation* distributions that would be independent of the *production* stage. The origin of such non-universality (that shows up at the level of $\alpha_s m^2 \ln m^2$ terms) may be traced back to the process dependent radiation of *hard* gluons,⁷

$$d\sigma \propto \omega_g \cdot d\omega_g \propto (1 - x) dx.$$

In practice we have to deal with a mixture of vector and axial production currents. In the pure axial case ζ should be substituted by

$$\zeta_A \equiv \frac{\sigma_{[A]}(v)}{\sigma_{[A]}(1)} = 1 - 4m^2 = v^2.$$

In addition, the $\zeta^{-1}(1 - x)$ term in (2.7) acquires an extra mass correction factor $(1 + 2m^2)$. Both this effect and the difference between ζ_V and ζ_A are proportional to $m^2 = (M/W)^2$. We conclude that

⁷ both the “soft” and “semi-soft” terms of the radiation spectrum, $\propto \omega_g^{-1} \cdot d\omega_g$ and $\propto 1 \cdot d\omega_g$, remain universal [24,25].

- the difference between the radiation spectra in V - and A -channels vanishes as $(1-v^2)$ in the relativistic case, while
- for non-relativistic quarks, $v \ll 1$, the axial contribution to the cross section is relatively suppressed as $A/V \sim v^2$.

Therefore (2.4)–(2.7) may be used in practice for the realistic $V+A$ mixture, in particular, at the Z^0 peak.

3 Hadronization and Infrared Finite α_s

In the QCD context the non-PT phenomena inevitably enter the game. It is important to stress however that the strong interaction not only determines the hadronization transition (1.1) but also affects to some extent the quark evolution stage: The high order effects embodied into the *running coupling* seem to undermine the very possibility of the PT analysis.

It is often believed that the large quark mass, $M \gg \Lambda$, provides a natural cut-off, which keeps the relevant space-time region compact enough to avoid the truly strong, non-PT interaction in a course of the quark evolution.

To illustrate the point we invoke a rough estimate that follows immediately from (2.6) and is valid for numerically large x values in the double-log approximation [7],

$$D(x; W, M) \propto (1-x)^{C_F \Delta \xi - 1}, \quad (3.1a)$$

with $\Delta \xi$ the characteristic evolution integral

$$\Delta \xi = \int_{(1-x)^2 M^2}^{(1-x) W^2} \frac{dk_\perp^2}{k_\perp^2} \frac{\alpha_s(k_\perp)}{\pi}. \quad (3.1b)$$

In the fixed coupling approximation we would get

$$D(x) \propto (1-x)^{\frac{C_F \alpha_s}{\pi} \ln \frac{W^2}{M^2} - 1} \cdot \exp \left\{ -\frac{C_F \alpha_s}{2\pi} \ln^2(1-x) \right\}. \quad (3.2)$$

In the small coupling regime, $C_F \frac{\alpha_s}{\pi} \ln \frac{W^2}{M^2} < 1$, this distribution exhibits a sharp peak at large x followed by a steep fall off in the $x \rightarrow 1$ limit due to the double logarithmic Sudakov suppression. Qualitatively similar shape for the heavy hadron spectrum due to $Q \rightarrow H_Q$ transition one expects from the parton model considerations [27] which have lead to the so called Peterson fragmentation function [9]

$$C_Q(x) = \frac{N}{x} \left[\frac{1-x}{x} + \frac{\epsilon_Q}{1-x} \right]^{-2}, \quad N = \frac{4\epsilon_Q^{1/2}}{\pi} \left[1 + \mathcal{O}(\epsilon_Q^{1/2}) \right]. \quad (3.3)$$

This function peaks at $1-x \approx \epsilon^{1/2} \ll 1$ leading to

$$\langle 1-x \rangle_{fragm} = \epsilon_Q^{1/2} \cdot \frac{2}{\pi} \left(\ln \epsilon_Q^{-1} - 1 \right) \left[1 + \mathcal{O}(\epsilon_Q^{1/2}) \right] \propto \epsilon_Q^{1/2}. \quad (3.4)$$

3.1 Peterson fragmentation function vs. integrated coupling.

One may single out effects of the non-PT momentum region by factorizing the D spectrum in the moment representation (2.6) into the product of the “safe” PT part and the “confinement” factor,

$$D_j = D_j \left[k_\perp^2 > \mu^2 \right] \times D_j^{(C)} . \quad (3.5a)$$

In other words, we split the radiator into two pieces corresponding to large and small transverse momentum regions ($t \approx k_\perp^2$ for x close to 1),

$$\frac{dw}{dx} = \frac{dw}{dx} \left[k_\perp^2 > \mu^2 \right] + \left\{ \frac{dw}{dx} \right\}^{(C)} \left[k_\perp^2 \leq \mu^2 \right] . \quad (3.5b)$$

This formal separation becomes informative if one is allowed to choose the boundary value μ well *below* the quark mass scale (e.g., $\mu = 1\text{GeV}$ providing $\mu/M \ll 1$ for the b quark case). Within such a choice only x close to 1 would contribute to $w^{(C)}$. For illustrative purposes let us neglect subleading μ/M effects and retain the most singular term only to get an estimate

$$\left\{ \frac{dw}{dx} \right\}^{(C)} \approx \vartheta \left(\frac{\mu}{M} - (1-x) \right) \int_{[(1-x)M]^2}^{\mu^2} \frac{dt}{t} a(t) \frac{2C_F}{1-x} + \dots \quad (3.6a)$$

One arrives at

$$\begin{aligned} \ln D_j^{(C)} &\approx \int_0^{\mu/M} dz \left[(1-z)^{j-1} - 1 \right] \int_{[zM]^2}^{\mu^2} \frac{dt}{t} a(t) \frac{2C_F}{z} \\ &= 2C_F \int_0^{\mu} \frac{dk}{k} \frac{\alpha_s(k)}{\pi} \int_0^k \frac{du}{u} \left[\left(1 - \frac{u}{M} \right)^{j-1} - 1 \right] . \end{aligned} \quad (3.6b)$$

It is important to stress that it is the first “confinement insensitive” factor of (3.5a) only that depends on W . Therefore, the ratio of the moments

$$D_j(W, M) / D_j(W_0, M) \quad (3.7a)$$

as a function of W and the heavy quark mass is expected to be an “infrared stable” PT prediction. Another message one receives observing the structure of the radiator (2.7) is that the ratio of the moments for *different* quarks,

$$D_j(W, M_1) / D_j(W, M_2) , \quad (3.7b)$$

should tend to a W -independent confinement sensitive (*sic!*) constant in the relativistic limit $W \gg M_1, M_2$.

We proceed with the estimate of the “confinement” factor (3.6b). As far as μ/M may be treated as a small parameter, for finite moments $j \sim 1$, $j\mu/M \ll 1$,

$$\ln D_j^{(C)} = -2C_F(j-1) \int_0^{\mu} \frac{dk}{M} \frac{\alpha_s(k)}{\pi} \left[1 + \mathcal{O} \left(\frac{jk}{M} \right) \right] \approx -2C_F(j-1) \frac{\mu_\alpha}{M} , \quad (3.8)$$

with

$$\mu_\alpha \equiv \int_0^\mu dk \frac{\alpha_s(k)}{\pi}. \quad (3.9)$$

In particular, for the energy losses, $j=2$, one has

$$\ln D_2^{(C)} \equiv \ln \langle x \rangle^{(C)} = -2C_F \frac{\mu_\alpha}{M} \left[1 + \mathcal{O}\left(\frac{\mu}{M}\right) \right], \quad \langle x \rangle^{(C)} = \exp \left\{ -2C_F \frac{\mu_\alpha}{M} \right\}. \quad (3.10)$$

If (3.8) were applicable for *all* j , the inverse Mellin transform would result in a singular distribution

$$D(x)^{(C)} = \delta \left(x - \langle x \rangle^{(C)} \right). \quad (3.11)$$

This singularity gets smeared when a proper treatment is given to the large j region. To this end one may use a simple expression that interpolates between (3.8) and the correct logarithmic asymptote of the “confinement radiator” in (3.6),

$$\ln D_j^{(C)} \approx -2C_F \int_0^\mu \frac{dk}{k} \frac{\alpha_s(k)}{\pi} \ln \left[1 + \frac{k}{M}(j-1) \right]. \quad (3.12)$$

As a result, a distribution emerges that peaks around $x = \langle x \rangle^{(C)}$ and is rather similar in shape to (3.3). The extreme $x \rightarrow 1$ asymptote is determined by the region of parametrically large moments $\langle j \rangle \propto (1-x)^{-1} \gg M/\mu$. It is different for two regimes:

$$\alpha_s(0) > 0, \quad \ln D_j^{(C)} \sim -C_F \frac{\alpha_s(0)}{\pi} \ln^2 \left(j \frac{\mu}{M} \right) \implies D(x) \propto \frac{\exp \left\{ -C_F \frac{\alpha_s(0)}{2\pi} \ln^2(1-x) \right\}}{1-x}; \quad (3.13a)$$

$$\alpha_s(0) = 0, \quad \ln D_j^{(C)} \sim -2C_F \Xi_0 \ln \left(j \frac{\mu}{M} \right) \implies D(x) \propto (1-x)^{2C_F \Xi_0 - 1}, \quad (3.13b)$$

where, in the latter case,

$$\Xi_0 \equiv \int_0^\mu \frac{dk}{k} \frac{\alpha_s(k)}{\pi} < \infty. \quad (3.14)$$

Reproducing the concrete behaviour of the Peterson function (3.3) in the large x limit, $C(x) \sim (1-x)^2$, would require $\Xi_0 = \frac{9}{8}$ in the second regime (3.13b). We conclude that the particle distribution originating from (3.6) is capable of reproducing the gross features of the popular Peterson fragmentation function (provided, naturally, that the notion of the infrared regular effective coupling is implanted in the PT-motivated “confinement” radiator).

An important message comes from comparing the energy losses that occur at the hadronization stage. Based on the pick-up hadronization picture, the characteristic parameter ϵ in (3.3) has been predicted to scale ^[9] as

$$\epsilon_Q \approx \left(\frac{m_q}{M} \right)^2 \propto M^{-2}, \quad (3.15)$$

(with m_q the quantity of the order of constituent light quark mass.) Confronting (3.4) that (up to a logarithmic factor) scales as $\sqrt{\epsilon_Q}$ with the PT prediction (3.10) we get

$$\langle 1-x \rangle_{fragm} \sim \sqrt{\epsilon_Q} \iff 1 - \langle x \rangle^{(C)} = 1 - \exp \left\{ -2C_F \frac{\mu_\alpha}{M} \right\} \approx 2C_F \frac{\mu_\alpha}{M},$$

which justifies the expected scaling law⁸.

It is worthwhile to remember that neither the Peterson function nor our PT-motivated “confinement” distribution is an unambiguously defined object. The former as an “input” for the evolution is by itself contaminated by gluon radiation effects at the hard scale $t \sim M^2$ that are present even at moderate $W \gtrsim 2M$. On the other hand, $D[k_\perp^2 \leq \mu^2]$ crucially depends on an arbitrarily introduced separation scale μ that disappears only in the product of the factors responsible for “PT” and “non-PT” stages (3.5a). Nevertheless, bearing this in mind, one may still speak of a direct correspondence between these two quantities, namely, $C(x)$ in the j representation and $D_j^{(C)}$ as given by (3.6).

This means that instead of convoluting phenomenological $C(x)$ with the W -dependent “safe” evolutionary quark distribution one may try to use consistently the pure PT description that would place no artificial separator between the two stages of the hadroproduction. From the first sight, one gains not much profit substituting one non-PT object — the phenomenological fragmentation function $C(x)$ — by another unknown, namely, the behaviour of the effective long-distance interaction strength $\alpha_s(k)$ (at, say, $k \lesssim 2\text{GeV}$). There is, however, an important physical difference between the two approaches: α_s should be looked upon as an *universal* process independent quantity. Therefore quite substantial differences between inclusive spectra of c- and b- flavoured hadrons should be under complete control according to the explicit quark mass dependence embodied in the PT formulae.

3.2 Modeling the coupling.

To study *infrared sensitivity* of PT results one can try different shapes of the effective coupling or, equivalently, different ways to extrapolate the characteristic function

$$\xi(Q^2) = \int^{Q^2} \frac{dk^2}{k^2} \frac{\alpha_s(k)}{\pi} + \text{const} \quad (3.16)$$

to the “confinement” region of small Q^2 . Using the one-loop expression for the coupling,

$$\frac{\alpha_s^{(1)}(k)}{\pi} \equiv 2a^{(1)}(k^2) = \frac{4}{b \ln(k^2/\Lambda^2)}; \quad b = \frac{11}{3}N_c - \frac{2}{3}n_f, \quad (3.17)$$

for ξ one gets

$$\xi^{(1)}(k^2) = \frac{4}{b} \ln \ln \frac{k^2}{\Lambda^2} + \text{const}, \quad (3.18)$$

which expression is defined only for $k > \Lambda$.

For the two-loop effective coupling we use the standard approximate expression

$$\alpha_s^{(2)}(k) = \alpha_s^{(1)}(k) \left(1 - \frac{b_1 \ln \ln(k^2/\Lambda^2)}{4\pi b} \alpha_s^{(1)}(k) \right) \quad (3.19a)$$

⁸Similar behaviour was advocated recently by R.L. Jaffe and L. Randall [28] who have exploited the difference between the hadron and the heavy quark masses as a small expansion parameter.

with

$$b_1 = \frac{34}{3} N_c^2 - \left(\frac{10}{3} N_c + 2C_F \right) n_f \quad (3.19b)$$

and $\alpha_s^{(1)}$ given by the one-loop formula (3.17). Analytic expression for ξ then reads

$$\xi^{(2)}(k^2) = \frac{4}{b} \left(\ln L + \frac{b_1 \ln L + 1}{b^2} \frac{1}{L} \right) + \text{const} ; \quad L \equiv \ln \frac{k^2}{\Lambda^2} . \quad (3.20)$$

3.2.1 *F*-model.

The simplest prescription which we refer below as the *F*-model consists of *freezing* the running coupling near the origin. One follows the basic PT dependence given by either (3.17) or (3.19a) down to a certain point k_c^2 where the coupling reaches a given value

$$\frac{\alpha_s(k_c)}{\pi} = A , \quad (3.21a)$$

and then keeps this value down to $k^2 = 0$. ξ then takes the form

$$\begin{aligned} &= \xi(k^2) - \xi(k_c^2) , \quad k^2 > k_c^2 ; \\ \xi(k^2) &= A \ln \left(k^2 / k_c^2 \right) , \quad k^2 < k_c^2 , \end{aligned} \quad (3.21b)$$

with k_c related to A by (3.21a).

3.2.2 *G*-model.

The set of G_p -models (Generalized shift models) gives another more flexible example for the trial effective coupling. It emerges when one regularizes the evolution function (3.18) as follows,

$$\xi^{(1)}(k^2) = \frac{4}{b} \ln \ln \left(\frac{k^{2p}}{\Lambda^{2p}} + C_p \right) + \text{const} , \quad C_p \geq 1 , \quad (3.22a)$$

which corresponds to the effective coupling

$$\frac{\alpha_s^{(1)}(k)}{\pi} \equiv \frac{d \xi^{(1)}(k^2)}{d \ln k^2} = \left[\frac{k^{2p}}{k^{2p} + C_p \Lambda^{2p}} \right] \cdot \frac{4}{b} \frac{p}{\ln(k^{2p}/\Lambda^{2p} + C_p)} . \quad (3.22b)$$

This expression preserves the perturbative asymptotic form (3.17) up to power corrections Λ^{2p}/Q^{2p} . Notice that the effective coupling (3.22b) with $C_p = 1$ has a finite limit $\alpha_s(0)/\pi = 4p/b$, while for $C_p > 1$ it vanishes in the origin.

For the two-loop coupling one substitutes in (3.20)

$$L \implies L_p = \frac{1}{p} \ln \left(\frac{Q^{2p}}{\Lambda^{2p}} + C_p \right) , \quad (3.23a)$$

which results in

$$\frac{\alpha_s^{(2)}(k)}{\pi} \equiv \frac{d \xi^{(2)}(k^2)}{d \ln k^2} = \left[\frac{k^{2p}}{k^{2p} + C_p \Lambda^{2p}} \right] \cdot \frac{4p}{b L_p} \left(1 - \frac{b_1}{b^2} \frac{\ln L_p}{L_p} \right). \quad (3.23b)$$

Trial shapes of the effective coupling in the G_2 model (G -model with $p=2$ and the two-loop α_s with $n_f = 5$ massless flavours) are displayed in Fig.1 for different values of the parameter C_2 . Crosses mark the curve that provides the best fit to mean energy losses (see below).

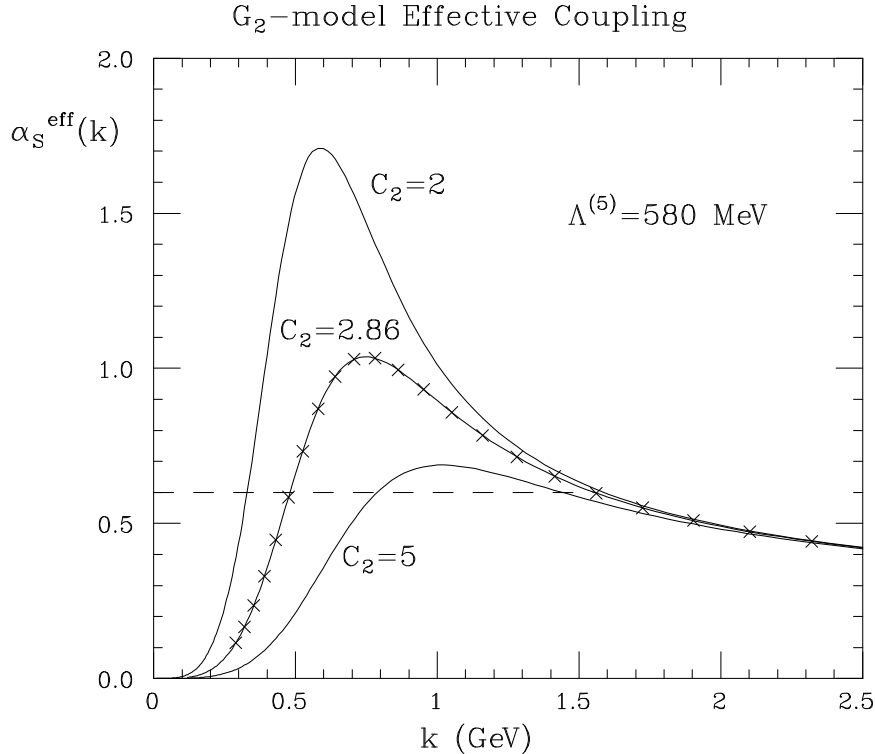


Figure 1: Trial shapes of α_s^{eff} in the G_2 model (two-loop, $n_f = 5$). Marked by crosses is the best-fit coupling. For comparison the best-fit F -model coupling ($A=0.19$) is shown with dashed line.

3.2.3 Quark Thresholds.

When it comes to an accurate account of heavy quark thresholds in α_s we modify the logarithmic denominator of $\alpha_s^{(1)}(k^2)$ in (3.19a) according to (2.19) as follows

$$b_{[n_f=5]} \ln \frac{k^2}{\Lambda^2} \implies b_{[n_f=3]} \ln \frac{k^2}{\Lambda^2} - \frac{2}{3} \left[\Pi \left(1 + \frac{4M_c^2}{k^2} \right) + \Pi \left(1 + \frac{4M_b^2}{k^2} \right) \right] \quad (3.24a)$$

with

$$\Pi(v^2) = \frac{v(3-v^2)}{2} \ln \frac{1+v}{1-v} + v^2 - \frac{8}{3}. \quad (3.24b)$$

Given infrared regular behaviour of α_s^{eff} , numerical evaluation of the inverse Mellin transform (2.4) with the PT radiator (2.7) becomes straightforward. Inclusive energy heavy quark spectrum obtained along these lines is concentrated (has a sharp maximum) near $x_Q = 1$ at $W \geq 2M$ and softens due to gluon bremsstrahlung effects with W increasing. Similar softening one achieves increasing radiation intensity in the PT domain (by taking a larger value of Λ) and/or at small momentum scales (by varying “confinement parameter” of the model; larger A , smaller C_p).

Since available experimental information on differential heavy quark spectra is rather scarce at present (and possibly contradictory), we restrict ourselves by considering the *mean energy losses* which, as we have discussed above, can be studied to quantify the influence of non-PT effects.

The value of $\langle x_Q \rangle \equiv D_2(W, M)$ shows up quite a strong variation with A/C . However, from the general factorization argument (3.7a) one would expect the *energy dependence* of $\langle x_Q \rangle$ to stay well under PT control. As demonstrated in [32], the normalized quantity

$$\langle x_Q \rangle(W) / \langle x_Q \rangle(W_0) \quad (3.25)$$

is indeed practically insensitive to the variation of the “confinement parameter” of the model. Therefore the ratio (3.25) may be looked upon as an *infrared stable* quantity suitable for measuring Λ as has been suggested by P.Mättig [1].

Position of the peak in the energy distribution seems to give another less trivial example of a stable prediction. Once again, as in the case of $\langle x_Q \rangle$, the *absolute* value of the peak position depends strongly on the chosen A value. At the same time the *normalized* quantity $x_{\text{peak}}(W) / x_{\text{peak}}(W_0)$ exhibits much weaker A/C -dependence than the PT-controlled dependence on Λ [7,8].

Thus the W -evolution (scaling violation) in quark energy losses $\langle x_Q \rangle(W)$ allows one to extract the scale parameter Λ which value proves to be practically insensitive to the adopted scheme of α_s^{eff} extrapolation. At the same time the *absolute* values of $\langle x_Q \rangle$ are quite sensitive to the gross effective radiation intensity below 1–2GeV which makes it possible to quantify corresponding “confinement parameter” of the scheme and, thus, the shape of the coupling.

Worthwhile to notice that there is a natural theoretical scale the “measurement” of α_s^{eff} below 1–2GeV to be compared to. As shown by Gribov [29], in the presence of light quarks colour confinement occurs when the effective coupling (parameter A of the F -model) exceeds rather *small* critical value

$$A > \left\{ \frac{\alpha_s}{\pi} \right\}^{\text{crit}} = C_F^{-1} \left[1 - \sqrt{\frac{2}{3}} \right] \approx 0.14. \quad (3.26)$$

Thus, within the Gribov confinement scenario an interesting possibility arises. Namely, if phenomenological α_s^{eff} extracted from the data does exceed α_s^{crit} but remains numerically small this would provide a better understanding of the PT approach to multiple hadroproduction in hard processes.

4 Numerical Analysis of Energy Losses

In this Section we compare experimental data with the generalized PT prediction which embodies the notion of the infrared regular effective QCD coupling. As an input we take the world average

values ^[1] of $\langle x_Q \rangle$ listed in Table 1.

process	$W_{cm}(\text{GeV})$	$\langle x_Q \rangle$
1.	10.4	0.727 ± 0.014
2. $c \rightarrow D^* + \dots$	30	0.587 ± 0.015
3.	91	0.508 ± 0.009
4. $c \rightarrow \ell + \dots$	57.8	0.541 ± 0.036
5. $c \rightarrow \ell + \dots$	91	0.522 ± 0.022
6. $b \rightarrow \ell + \dots$	29–35	0.789 ± 0.022
7. $b \rightarrow \ell + \dots$	91	0.699 ± 0.009

Table 1: Experimental measurements of $\langle x_Q \rangle (W, M)$

Errors have been evaluated by taking statistical and systematic errors in quadrature. First 3 entries stand for the direct production of D^* mesons at different centre-of-mass energies; the last 4 data for the mean *quark* energy have been extracted by unfolding the inclusive lepton (e, μ) spectra from heavy Q decays.

As mentioned above, the PT approach advocated in this paper can not pretend to fully describe *exclusive* heavy hadron spectra (with D^* an example). Our treatment of the hadronization stage that implicitly appeals to duality arguments makes it plausible to rather apply this approach to inclusive quantities such as the lepton energy distributions. Nonetheless, for lack of anything better, we take the measured mean energy of D^* as a representative of $\langle x_Q \rangle$ to be compared directly with the PT motivated prediction for the quark energy losses.

The preliminary analysis has shown ^[7,8] that an independent fitting of the D and L (epton) data results in the best-fit curves $A_D(\Lambda)$ and $A_L(\Lambda)$ that *cross* just at the best-fit value of Λ . This was the observation that motivated us to look upon α_s^{eff} as a process independent quantity to confront the c and b measurements 1–7 with a unique one-parameter PT prediction⁹.

Hereafter we fix heavy quark masses to be

$$M_c = 1.5 \text{ GeV}, \quad M_b = 4.75 \text{ GeV}. \quad (4.1)$$

(Sensitivity to the b –quark mass will be discussed below.)

4.1 Fitting mean quark energies.

Fig.2 shows the quality of the fit to 7 separate data of the Table 1 together with the total χ^2 as a function of $\Lambda^{(5)}$ in the G_2 -model with $C_2 = 2.86$ (the best-fit value). Some explanation is in order. In this Figure (and similar plots below) for each datum the ratio is displayed

$$\frac{\text{theor.} - \text{exp.}}{\text{exp.error}} \quad (4.2)$$

⁹in spite of the fact that such a naïve approach suggests the same theoretical expectation for the two physically different data # 3 and # 5.

against the right vertical scale. Dashed horizontal lines mark 1σ levels for each single datum. The two curves (which should be read out against the left scale) show the squared deviation of the points (4.2) from the median, that is, total χ^2 . The solid curve sums up all 7 data, while the dash-dotted one accumulates the “high W ” data only. The “high W ” sample we define excluding the entries #1 and #6 which correspond to the quark mass-to-energy ratios

$$M/E \approx M_c/5\text{GeV} \sim M_b/15\text{GeV} \approx 1/3.$$

These two entries are subject to significant non-relativistic corrections. The fact that the two fits are consistent is good news: it shows that the non-relativistic effects have been properly taken into account¹⁰ in the PT radiator (2.7).

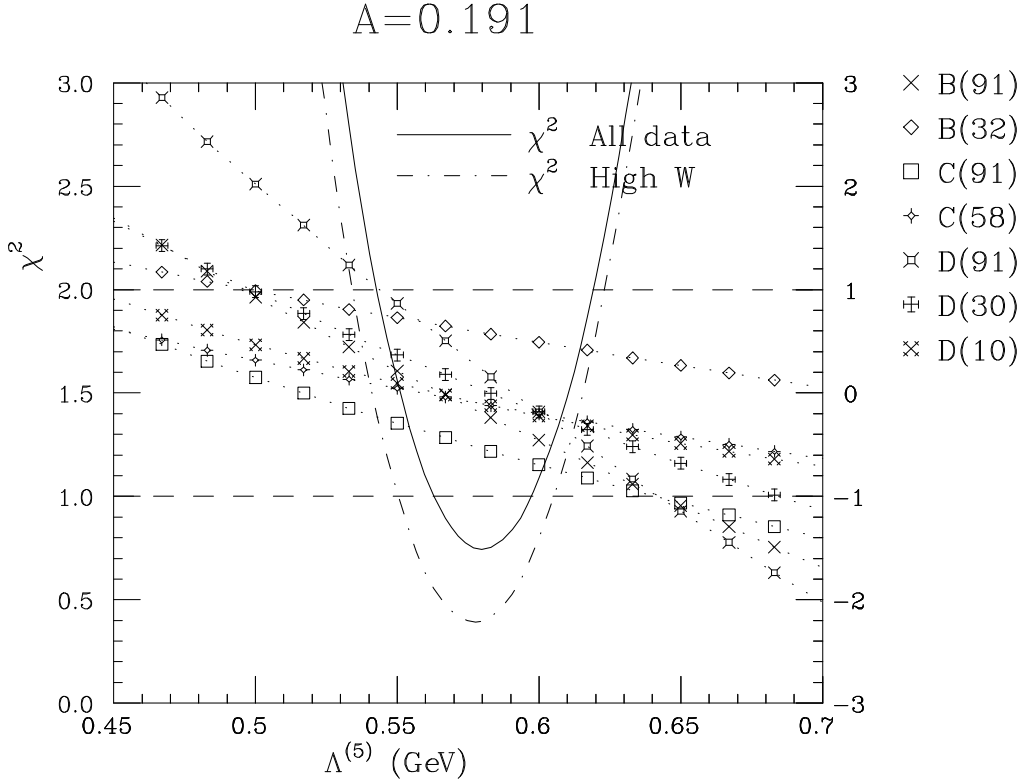


Figure 2: Λ -dependence of the F -model fit to mean energy losses (two-loop α_s^{eff} with $n_f = 5$). The right scale shows normalized deviation between a theoretical prediction and an experimental datum (4.2). Dashed lines mark the 1σ band. Solid and dash-dotted lines show the values of χ^2 (against the left scale) for all data and the high- W data sample correspondingly.

Fig.3 demonstrates sensitivity of PT description to the “confinement parameter”. Here we have chosen the G_2 -model for a change. The first thing to be noticed is that with the best-fit

¹⁰the relativistic version of (2.4–7) reported earlier [7] failed to properly embody the “ b at 32” datum # 6

parameter $C_2 = 2.86$ one obtains the same value $\Lambda^{(5)} \approx 580$ MeV, comparable quality of the fit $\chi^2_{\min} \approx 0.7$ and even the same dynamics of each of 7 data as in the above F -model description (Fig.2). In the upper part of this plot two marginal values of C_2 are also shown which correspond to one standard deviation from the total 7-fit: $\chi^2_{\min}(2.53) = \chi^2_{\min}(3.21) = \chi^2_{\min}(2.86) + 1$.

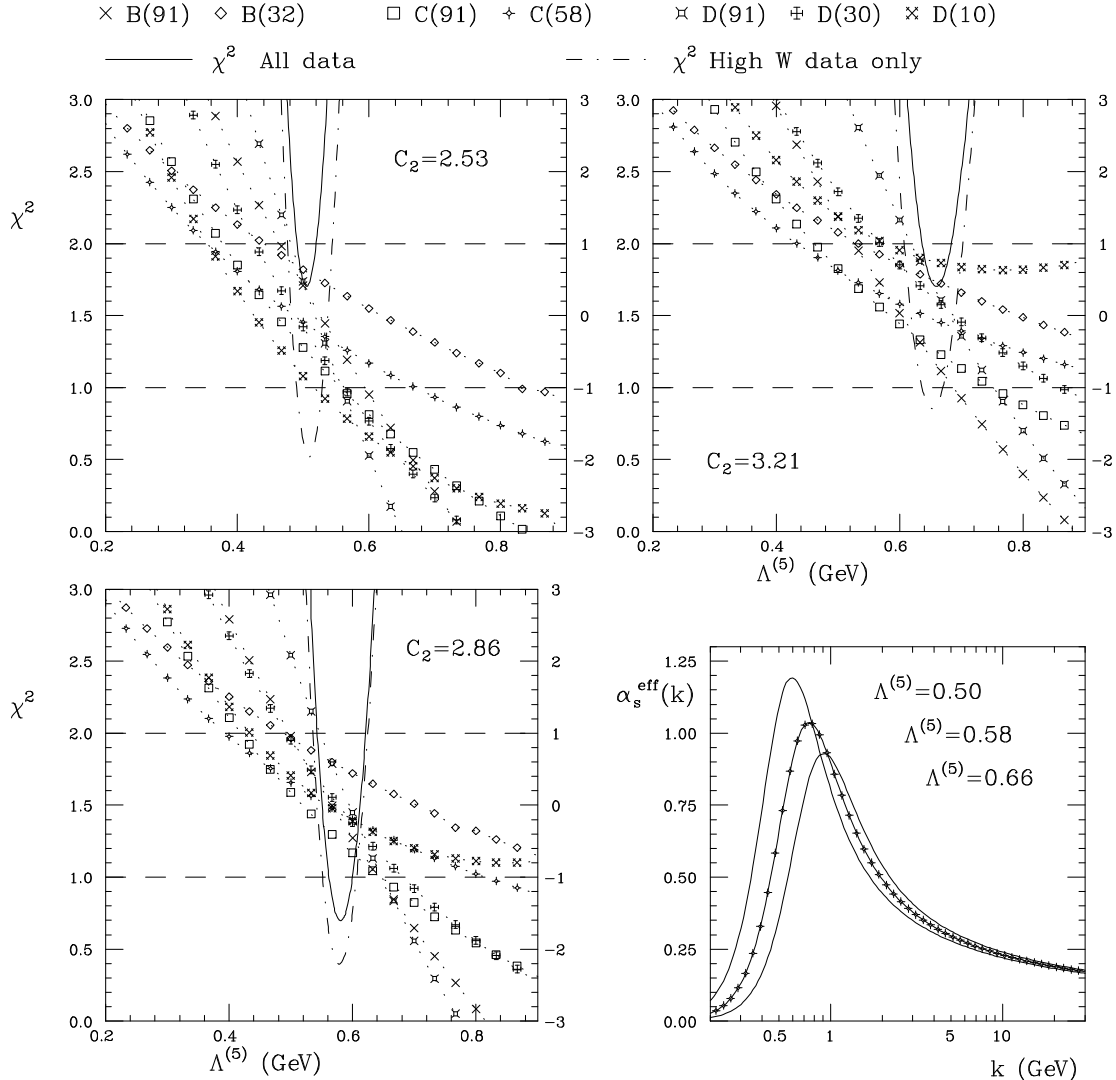


Figure 3: On sensitivity of the G_2 -model fit to the shape of α_s^{eff} in the origin (two-loop, $n_f = 5$). The values of C_2 in the upper plots correspond to one standard deviation from the best-fit (bottom-left). Bottom-right graph displays the margin in low momentum behaviour of α_s^{eff} .

In Fig.4 comparison is made of the quality of the fits within different models for the effective coupling (two-loop, $n_f = 5$). For each value of Λ the A/C parameter has been adjusted to minimize the error (one-parameter fit). The upper scale shows corresponding values of $\alpha_{\overline{\text{MS}}}$ at LEP recalculated from α_s^{eff} with use of the relation (2.17b).

It is worthwhile to notice some peculiarity of the G_1 -model. This model is “too soft” in a sense that it induces the *negative* preasymptotic power term $\propto k^{-2}$ in $\alpha_s^{\text{eff}}(k)$, which correction suppresses α_s^{eff} in a relatively high momentum region.

Fig.5 illustrates this peculiarity. Here the couplings corresponding to the best-fit A/C values for $\Lambda^{(5)} = 580$ MeV are compared. Solid lines (F, G_{2-4}) correspond to $\chi^2 \approx 0.7$. In the G_1 -model shown by dash-dotted line ($\chi^2 \approx 1.2$) α_s^{eff} stays noticeably smaller above 1.5 GeV before the perturbative logarithmic regime sets up and all the models merge.

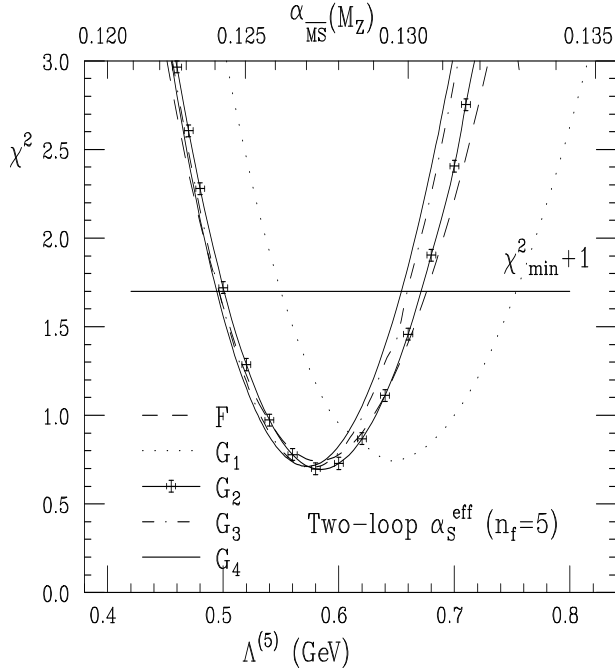


Figure 4: One-parameter fits to energy losses within different models for α_s^{eff} .

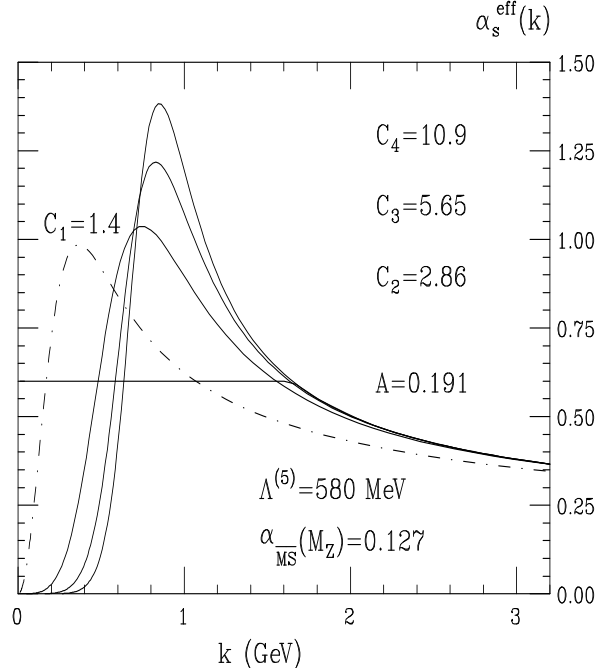


Figure 5: Best-fit α_s^{eff} for $\Lambda^{(5)} = 580$ MeV. G_1 -model underestimates radiation above 1.5 GeV.

As a result, to compensate for reduced radiation intensity the best-fit Λ value (and thus $\alpha(M_Z)$) within the G_1 -model tends to be larger compared to “sharp” models F, G_2, \dots

Leaving G_1 aside we conclude that both the quality of the fit and the value of Λ the “sharp” models point at, hardly exhibit any model dependence. From Fig.4 (see also Fig.3) we deduce

$$\Lambda^{(5)} = 580 \pm 80 \text{ MeV}. \quad (4.3a)$$

Being translated into the $\overline{\text{MS}}$ parameter this gives

$$\alpha_{\overline{\text{MS}}}(M_Z) = 0.127 \pm 0.003. \quad (4.3b)$$

The error here is purely statistical (one standard deviation).

In what follows we shall be using the 0.003 shift in $\alpha_{\overline{\text{MS}}}(M_Z)$ induced by the G_1 -model (see Fig.4 and Table 2 below) as a rough estimate of systematic uncertainty due to possible “soft” preasymptotic power effects in the running coupling.

Fig.6 demonstrates consistency of the total G_2 -model fit with fits to various subsets of data: D^* (items 1–3 of Table 1), “leptons” (4–7), high W (items 2–5, 7). Here χ^2 is plotted against the reference value $\alpha_{\overline{\text{MS}}}(M_Z)$.

D^* data are more restrictive since they have smaller experimental errors than inclusive lepton measurements. Low- W points $b \rightarrow \text{lepton} + \dots$ at 32 (#6) and, especially, D^* at 10 (#1) are quite important as they provide lever arm for scaling violation. Inclusion of these two measurements does not spoil the fit, $\chi^2/5$ (total fit) $\approx \chi^2/3$ (high- W), but increases its quality reducing statistical error by factor 2.

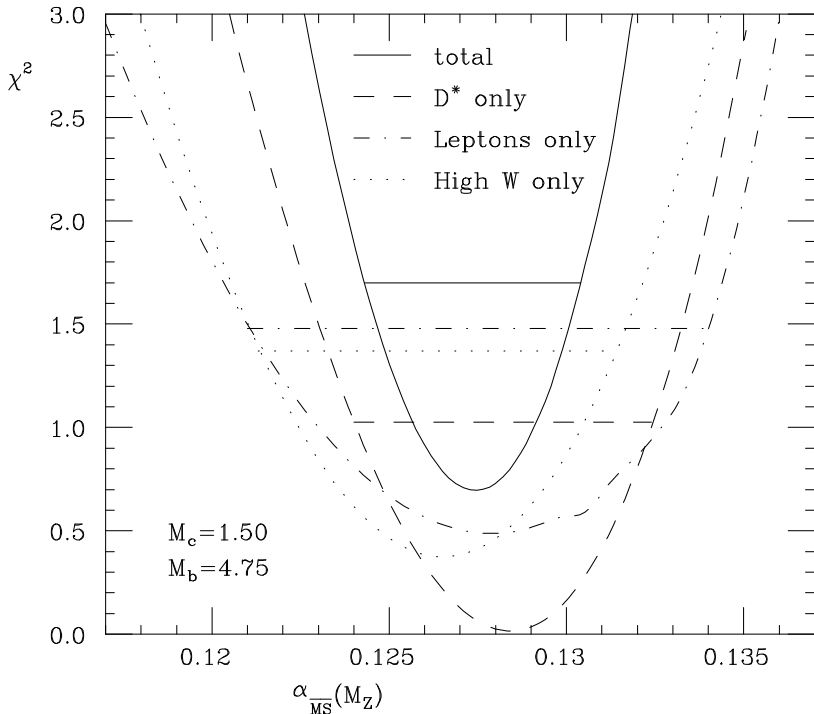


Figure 6: On consistency between the fits to different subsets of data on mean energy losses (two-loop, $n_f=5$). Horizontal lines mark one standard deviation levels.

4.2 Energy ratios and Λ determination.

In **Fig.7** results of the G_2 -model fit to the *ratios* of $\langle x_Q \rangle$ at different energies are shown. Solid curves accumulate the squared errors in the description of four ratios: $D^*(91)/D^*(10)$, $D^*(91)/D^*(30)$ and two ratios from leptonic quark decays, $C(91)/C(58)$ and $B(91)/B(32)$. As we have discussed above, one expects such ratios to be protected against our ignorance about the confinement physics. Indeed, a rather high stability in the quality of the fit inside a huge range of variation of the “confinement parameter” C_2 is seen. Bottom-right insertion displays corresponding shapes of α_s^{eff} . Within the chosen interval of C_2 the characteristic value of \bar{A} (4.6)

varies from 0.09 ($C_2 = 10$, $\Lambda = 0.7$) up to 0.41 ($C_2 = 1.4$, $\Lambda = 0.5$) that is changes by factor 2 in both directions around the value 0.19 (4.6b) that we have obtained describing *absolute* energy losses.

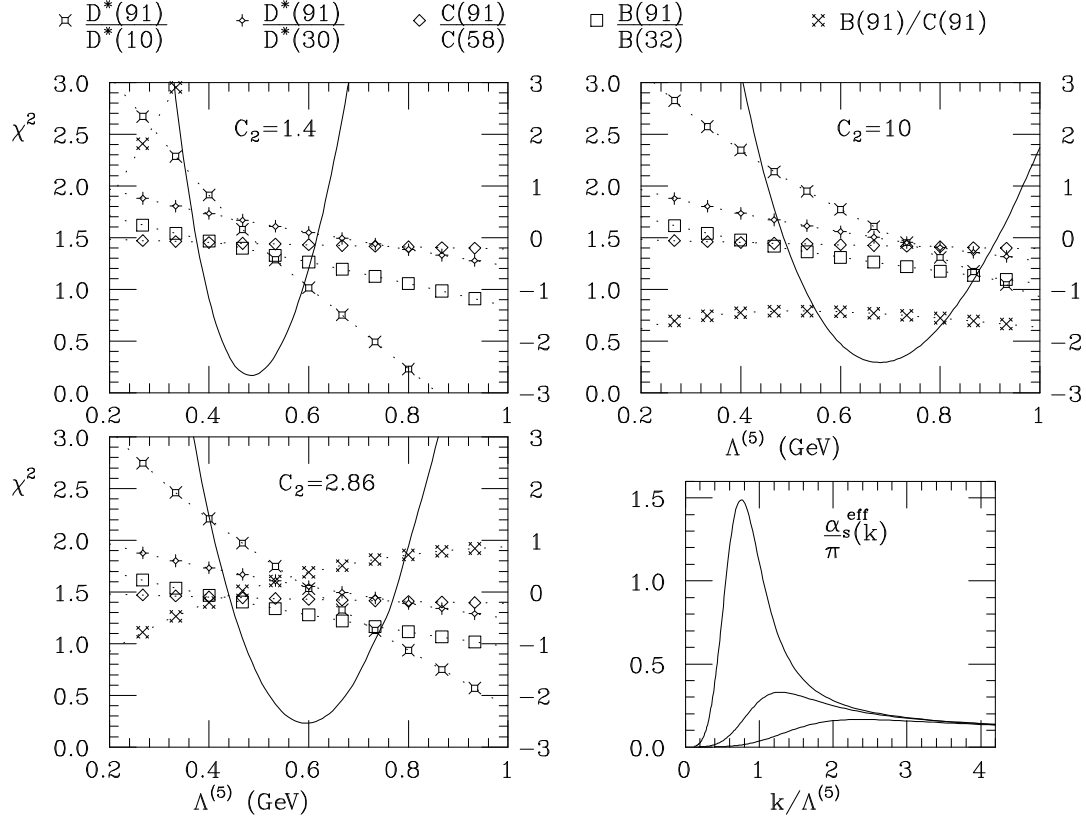


Figure 7: C_2 -dependence of energy ratios (G_2 -model, two-loop, $n_f=5$) with χ^2 for the first four ratios shown by solid lines and corresponding shapes of α_s^{eff} (bottom-right). The ratio $B(91)/C(91)$ not belonging to the fit exhibits strong C_2 -dependence, contrary to generic c/c and b/b ratios.

Also shown in Fig.7 is the mixed bottom-to-charm ratio $B(91)/C(91)$. This one does not belong here and, contrary to the generic c/c and b/b quark ratios, strongly depends on C_2 as expected.

We observe that three of four generic ratios show up no variation with C_2 at all. It is the ratio $D^*(91)/D^*(10)$ only that induces some *negative* correlation between \bar{A} and Λ : the latter moves to larger values with decrease of low-scale interaction intensity. Such a systematic drift is natural: charm quark mass is too small to completely protect the normalization point $D^*(10)$ against *W-dependent* (sic!) confinement effects at total energy as low as 10 GeV. At the same time the first ratio dominates in the fit while experimental accuracy of three others is not sufficient at present to provide a direct safe way of measuring the Λ parameter.

Roughly one might present the result of fitting quark energy ratios as

$$\Lambda^{(5)} = 0.60 \pm 0.15 \text{ (stat.)} \pm 0.10 \text{ (syst.)} . \quad (4.4a)$$

If statistical and systematic errors in Fig.7 were uncorrelated (which is not the case), (4.4a) would correspond to

$$\alpha_{\overline{\text{MS}}}(M_Z) = 0.128 \pm 0.007. \quad (4.4b)$$

For the time being it will suffice to conclude that determination of $\Lambda^{(5)}$ from quark energy ratios is consistent with that from absolute energy losses, cf. (4.3).

4.3 On bottom quark mass.

Fig.8 illustrates sensitivity of the total 7-fit to the bottom quark mass. Here we have fixed $M_c = 1.5$ GeV and looked for minimal χ^2 with respect to variation of A/C_2 (1-parameter fit) for given Λ and M_b .

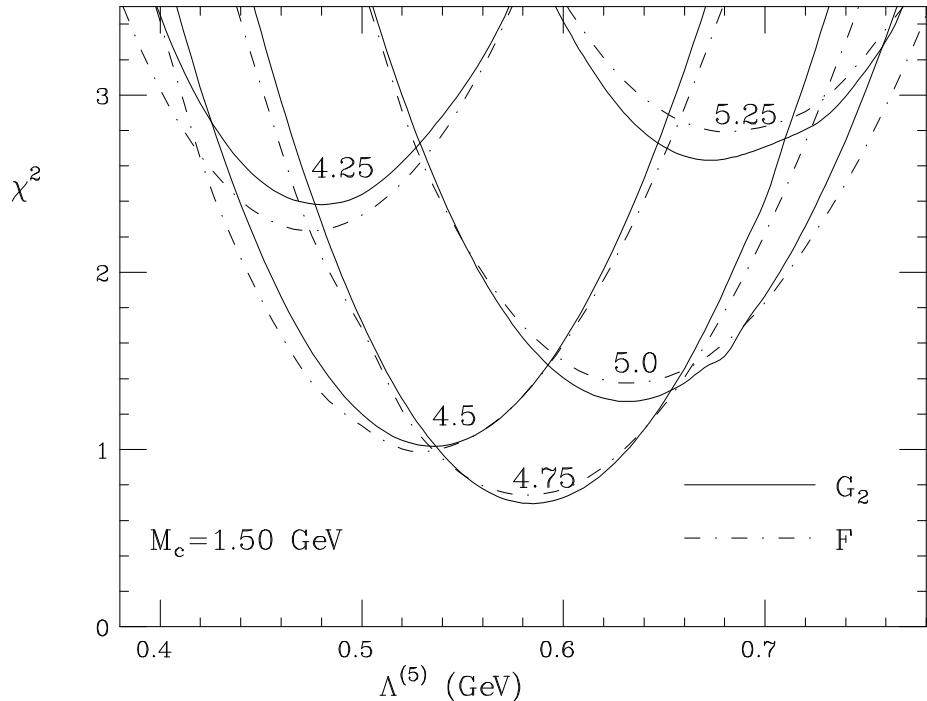


Figure 8: M_b dependence. Fits within F and G_2 models are shown (two-loop, $n_f=5$.)

Quark mass dependence of the spectrum (2.4)–(2.7) and, thus, of energy losses is basically logarithmic (apart from non-relativistic corrections $(M/W)^2$ and “confinement” effects μ_α/M). Nevertheless, a certain range of “preferable” bottom quark masses may be read out from Fig.8. Within one standard deviation (G_2 -model)

$$M_b = 4.73 \pm 0.38 \text{ GeV}. \quad (4.5)$$

A better understanding of the nature of the mass parameter M as it enters PT formulae is needed before such an analysis may be used for “measuring” bottom quark mass.

As for now, one finds satisfaction in noticing that the value $M_b = 4.75\text{GeV}$ we have been using throughout this paper [31] does fit nicely into the PT picture of mean energy losses.

4.4 Integrated coupling as invariant of the fit.

Being free to play around with the detailed shape of α_s^{eff} in the origin, one finds it necessary at the same time to fix some characteristic measure of the radiation intensity in the non-PT momentum region. Fig.5 suggests trying an *area* under the curve for an invariant parameter of the fit. The result is quite impressive: areas under the G_{2-4} and F couplings are practically indistinguishable. Introducing

$$\bar{A}(\mu) \equiv \frac{1}{\mu} \int_0^\mu dk \frac{\alpha_s^{\text{eff}}(k)}{\pi}, \quad (4.6a)$$

we get (with one standard deviation error estimated from the G_2 -model margin, see Fig.5)

$$\bar{A}(2\text{GeV}) = 0.190 \pm 0.010. \quad (4.6b)$$

This integral measure not only proves to be quite stable against the choice of *low*-momentum regularization but also resistant to different approximations for the *high*-momentum tail of $\alpha_s^{\text{eff}}(k)$.

Table 2 accumulates characteristics of various 7-fits and demonstrates an amusing stability of the value (4.6b). This justifies the qualitative expectation of subsection 3.1 that it is the integral of the coupling as a characteristic measure of confinement (hadronization) effects in inclusive energy spectra, μ_α of eq.(3.9), that is responsible for the low-momentum contribution to mean energy losses.

Thus we find empirically that the characteristic integral (4.6) turns out to be a *fit-invariant* quantity which one has to keep fixed to describe the absolute values of energy losses. As pointed out by V.N. Gribov, it can be looked upon as the long-distance contribution to the QCD field energy of a heavy quark. It is worthwhile to notice that such an integral appears in the relation between the running heavy quark mass at scale μ and the pole mass [30]

$$M^{\text{pole}} - M(\mu) = \frac{8\pi}{3} \int_{|\vec{k}| < \mu} \frac{d^3k}{(2\pi)^3} \frac{\alpha_s(k)}{k^2} = C_F \int_0^\mu dk \frac{\alpha_s(\kappa)}{\pi} \equiv C_F \mu_\alpha. \quad (4.7)$$

4.5 Two-loop α_s^{eff} with heavy quark thresholds and $\alpha_{\overline{\text{MS}}}$ determination.

It is important to notice that the different approximations for the high-momentum tail of α_s^{eff} listed in Table 2 provide similar quality fits and preserve the \bar{A} value but, at the same time, lead to systematically different values of $\alpha_{\overline{\text{MS}}}(M_Z)$. Fig.9 helps to relate the values of Λ parameter for different approximations for the running α_s^{eff} to the reference value $\alpha_{\overline{\text{MS}}}(M_Z)$.

In the problem under consideration one probes the coupling at M_Z scale only indirectly. For the first thing, “half” of the data belong to smaller W s. Moreover, even when the LEP measurements are concerned, the main contribution to energy losses originates from a broad logarithmic integral of $\alpha_s^{\text{eff}}(k)$ running from $k \lesssim M_Q$ up to $k \lesssim M_Z$, so that momenta just above M_b (as well as between M_c and M_b) play quite an essential role. The reference values of $\alpha_{\overline{\text{MS}}}$

Model for α_s^{eff}	Best-fit parameter	Λ (MeV)	$\alpha_{\overline{\text{MS}}}(M_Z)$	χ^2 5 d.o.f.	Integral \bar{A} (4.6b)
2-loop, with c, b thresholds; $\Lambda^{(3+2)}$	$A = 0.184$	730 ± 95	0.125	0.66	0.184
	$C_2 = 2.48$	725 ± 85	0.125	0.64	0.191
	$C_3 = 4.41$	710 ± 80	0.124	0.66	0.193
	$C_4 = 7.79$	705 ± 80	0.124	0.68	0.194
	$C_1 = 1.38$	820 ± 100	0.128	0.69	0.189
2-loop, with 5 massless quarks; $\Lambda^{(5)}$	$A = 0.190$	585 ± 85	0.127	0.73	0.187
	$C_2 = 2.88$	585 ± 80	0.127	0.68	0.191
	$C_3 = 5.59$	575 ± 80	0.127	0.69	0.193
	$C_4 = 10.8$	575 ± 75	0.127	0.70	0.193
	$C_1 = 1.46$	655 ± 95	0.130	0.75	0.190
1-loop, with 3 massless quarks; $\Lambda_{\text{1-loop}}^{(3)}$	$A = 0.193$	480 ± 70	0.120	0.71	0.188
	$C_2 = 2.22$	485 ± 65	0.120	0.66	0.190
	$C_3 = 3.94$	480 ± 60	0.120	0.66	0.191
	$C_4 = 6.90$	480 ± 60	0.120	0.66	0.191
	$C_1 = 1.20$	515 ± 75	0.122	0.69	0.189
1-loop, with 5 massless quarks; $\Lambda_{\text{1-loop}}^{(5)}$	$A = 0.209$	310 ± 50	0.133	0.90	0.189
	$C_2 = 2.68$	315 ± 50	0.133	0.79	0.191
	$C_3 = 5.48$	315 ± 50	0.133	0.78	0.191
	$C_4 = 10.9$	315 ± 50	0.133	0.79	0.191
	$C_1 = 1.28$	330 ± 50	0.134	0.84	0.189

Table 2: Best 7-fits within various models for effective coupling. A/C , $\alpha_{\overline{\text{MS}}}$, χ^2 and \bar{A} are given for the central Λ values.

appearing in Table 2 emerge as a result of extrapolation from intermediate momentum scales that dominate in the fit. Such an extrapolation is sensitive to details of high-momentum behaviour of the running coupling. When n_f is taken smaller and/or the two-loop effects are being taken into account, α_s^{eff} becomes a steeper falling function of momentum and the resulting value of $\alpha_{\overline{\text{MS}}}(M_Z)$ decreases.

Even an account of heavy quark thresholds (which makes $\alpha_s^{\text{eff}}(k)$ a steeper function below $k \lesssim M_b$) drives down the $\alpha_{\overline{\text{MS}}}$ value. To demonstrate this effect we include Figs.10 and 11 showing quality of the PT description of absolute energy losses with account of the second loop and c, b quark threshold effects in the running coupling. In Fig.10 model dependence of the total 7-fit is shown (cf. Fig.4); Fig.11 collects fits to different subsets of data (cf. Fig.6).

Our conclusions about relative stability against the choice of low-momentum regularization model and about consistent description of leptonic, D^* and high- W data hold. From these plots one obtains (see also Table 2)

$$\Lambda^{(3+2)} = 0.720 \pm 0.080 \text{ (stat)} \pm 0.015 \text{ (syst)} \text{ GeV} , \quad (4.8a)$$

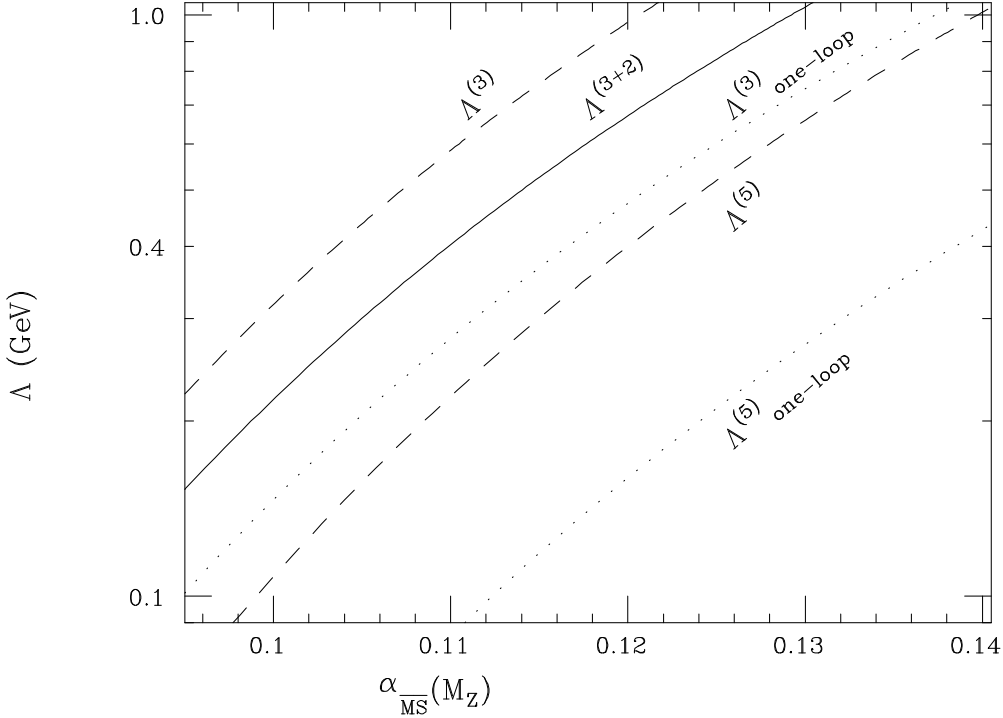


Figure 9: Relation between Λ and $\alpha_{\overline{\text{MS}}}(M_Z)$: one-loop (dotted), two-loop (dashed) for 3 and 5 massless quarks and the two-loop coupling with c, b quark thresholds (solid).

where we have singled out systematic uncertainty due to model dependence. This results in

$$\alpha_{\overline{\text{MS}}}(M_Z) = 0.125 \pm 0.003. \quad (4.8b)$$

It is important to stress that the second loop effects are there in the running coupling and n_f is not a free parameter: quarks (and their masses) are what they are. Therefore a huge interval of $\alpha_{\overline{\text{MS}}}$ values seen in Table 2 has nothing to do with actual theoretical uncertainty in determining this important datum.

Before we turn to discussion of systematic errors some comment is in order. It has to do with the number of acting quark flavours and will eventually give us an additional consistency check of the approach.

An attentive reader could have noticed that using 5-flavour running coupling seems to contradict the very logic of the present paper. Indeed, in Section 2 we constructed the energy distribution corresponding to *direct* production of a heavy quark Q . To do so we disregarded sea mechanism of heavy quark production and omitted the second loop anomalous dimension term related to $Q\overline{Q}Q\overline{Q}$ final states.

However, there is yet another subtle source of copious $Q\overline{Q}$ pairs, namely, the running coupling α_s^{eff} embodied into PT radiator. The way the coupling runs in theoretical expressions for inclusive characteristics depends on experimental setup: Veto on fermion pair production in the final state suppresses effective interaction strength at large momentum scales (QCD coupling decreases

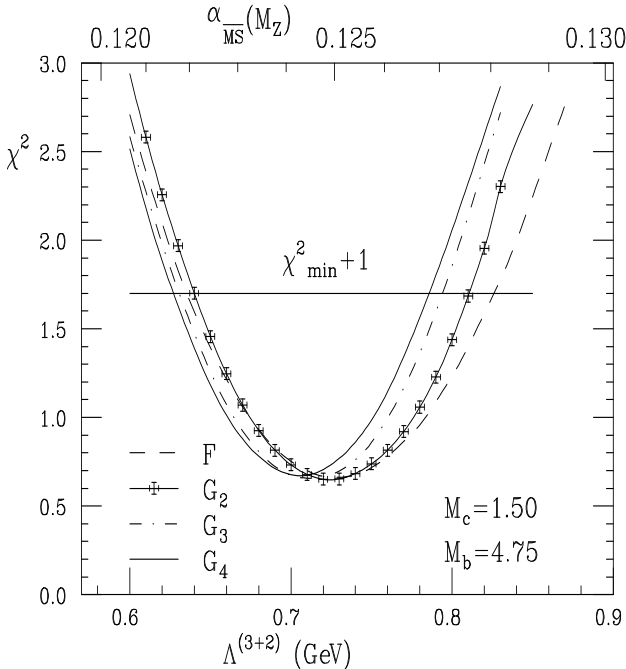


Figure 10: Quality of the total fits versus Λ (two-loop α_s^{eff} with c, b thresholds).

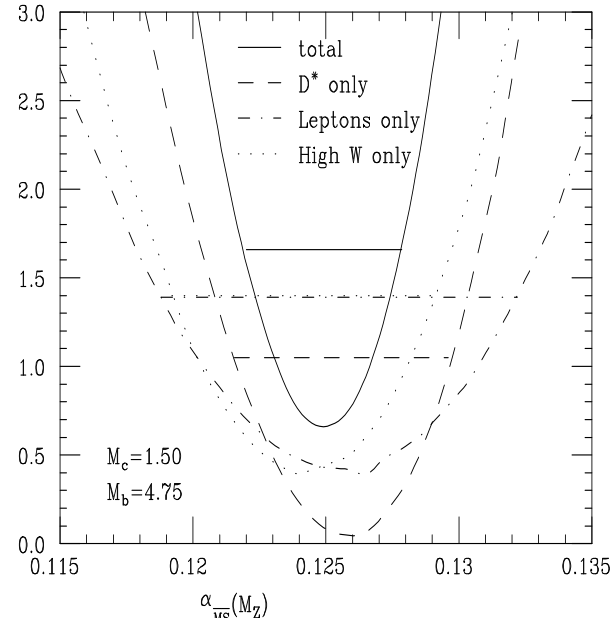


Figure 11: On consistency of G_2 -model fits to subsets of data (two-loop; c, b thresholds).

faster; an increase of α_{em} slows down). Therefore, to preserve the logic of the approach, we better make it clear that the use of $n_f = 3$ effective coupling which goes along with suppression of additional $c\bar{c}, b\bar{b}$ pairs is consistent with the reported result (4.8b).

In Fig.12 G_2 -model couplings are shown with the best-fit parameters Λ and C_2 listed in Table 3. As far as low momenta are concerned, variations due to n_f and one vs. two loops should be looked upon simply as different models for trial regularized coupling. All of them do the job. In particular, the 3-flavour α_s^{eff} which interests us at the moment (the last line of Table 3) does provide an excellent fit, $\chi^2/\text{d.o.f.} \approx 0.6/5$.

G_2 -model	n_f	$\Lambda^{(n_f)}$	C_2	χ^2	$\bar{A}(2\text{GeV})$	$\alpha_s^{\text{eff}}(2\text{GeV})$	$\alpha_s^{\text{eff}}(M_b)$	$\alpha_s^{\text{eff}}(M_Z)$	$\alpha_{\overline{\text{MS}}}(M_Z)$
+thresholds	3+2	725	2.48	0.65	0.191	0.530	0.303	0.135	0.125
1-loop	5	315	2.68	0.79	0.191	0.443	0.302	0.145	0.133
	4	395	2.43	0.72	0.191	0.463	0.303	0.139	0.126
	3	485	2.22	0.66	0.190	0.488	0.306	0.134	0.120
2-loop	5	585	2.88	0.69	0.191	0.494	0.303	0.138	0.128
	4	770	2.72	0.64	0.190	0.549	0.305	0.131	0.120
	3	935	2.56	0.62	0.190	0.608	0.305	0.124	0.112

Table 3: Characteristics of the best G_2 -model fits.

High stability of the \bar{A} value (4.6b) is confirmed once again. Moreover, one more interesting

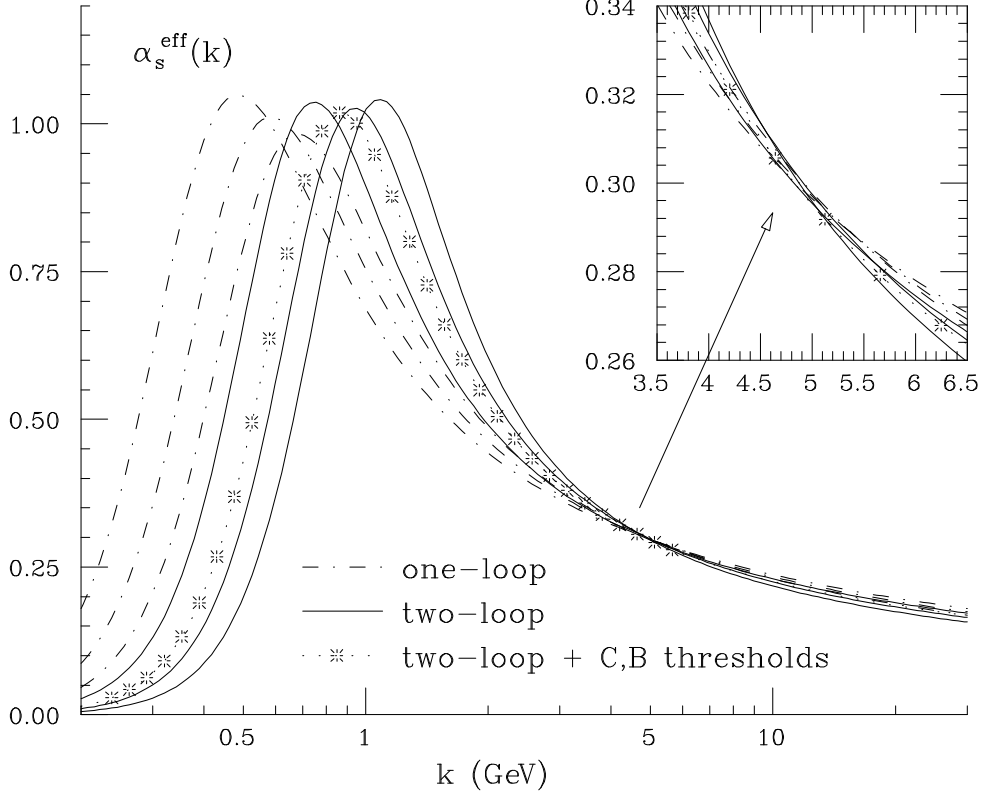


Figure 12: Best-fit G_2 -model effective couplings. $n_f = 5, 4, 3$ progress from left to right.

fit-invariant quantity emerges, namely, the value of the effective coupling at the bottom mass scale¹¹,

$$\alpha_s^{\text{eff}}(M_b) \approx 0.30. \quad (4.9)$$

The curves in Fig.12 are quite different below 2GeV, focus around 5GeV and diverge again at high momenta. The columns adjacent to the double-lined one in Table 3 illustrate this behaviour. In particular, the 3-flavour coupling continued to the LEP scale is substantially lower compared to the “3+2” coupling we have been using before (0.124 vs 0.135). However, it would be erroneous to read out $\alpha_{\overline{\text{MS}}} = 0.112$ from the last line of Table 3.

As we see, heavy flavours in α_s^{eff} are indeed irrelevant for the problem under consideration. However, they do contribute to the evolution of the standard QCD coupling. Therefore, having found the magnitude of α_s^{eff} at intermediate scales $k \sim 5$ GeV which dominate in the problem, one has to apply the 5-flavour evolution from ~ 5 up to 91 GeV aiming at extraction of the reference value $\alpha_{\overline{\text{MS}}}(M_Z)$.

Since the starting value $\alpha_s^{\text{eff}}(M_b) = 0.305$ practically coincides with that from the previous “3+2” analysis (0.303), so do the results. Choosing the starting point of high momentum ex-

¹¹since magnitude of α_s^{eff} around 5GeV $\gg \Lambda$ is insensitive to A/C and depends only on Λ , the same conclusion (4.9) follows from F and $G_{3,4}$ models

trapolation in between $k = M_b/2$ and $k = 2M_b$ leads to

$$\alpha_{\overline{\text{MS}}}(M_Z) = 0.125 \pm 0.003. \quad (4.10)$$

The, slightly inflated, error here is moderate, and the central value perfectly matches with the result of the previous analysis (4.8b) based on “3+2” coupling.

4.6 Systematic errors and prospects.

First of all, there is a problem of correspondence between theoretical prediction and the data. As we have stressed above, formulae of this paper were designed to describe mean energy of a primary quark produced in the e^+e^- annihilation vertex. We were treating experimental numbers as corresponding to direct $Q\overline{Q}$ production. We do not feel in a position to judge to what extent the experiments actually met such an expectation.

The good news is however that the bottom sector is safe in this respect: $g \rightarrow b$ sea component is vanishingly small at present, and so is charm production at low energies ^[33]. Therefore only LEP charm data should concern us here. Bearing this in mind it is important to notice that the D^* LEP datum #3 (which is the most precise measurement and therefore practically the only one vulnerable) does correspond to primary charm¹². MC modeling was used to subtract the gluon component (with an uncertainty included into experimental systematic error). Reliability of such a subtraction has been recently verified by the first OPAL measurement of the charm production via gluons ^[34].

Apart from this, one can think of the following sources of systematic error of $\alpha_{\overline{\text{MS}}}(M_Z)$ determination.

higher orders. **Estimate:** 0.002; **Comment:** optimistic.

Follows from analysis of approximate relation (2.17b) between physical coupling α_s^{eff} and $\alpha_{\overline{\text{MS}}}$ and of forceful exponentiation of α_s terms in the radiator (2.7). Apart from three-loop analysis, an exact $\mathcal{O}(\alpha_s^2)$ theoretical calculation of $\langle x_Q \rangle$ would be helpful.

power effects in $\alpha_s^{\text{eff}}(k > 2\text{GeV})$. 0.003; arbitrary (hopefully conservative).

Is based on comparison with the “soft” G_1 -model (see above). Variation within “hard” regularization models (F, G_{2-4}) is below 0.001 (see (4.8)). To gain quantitative theoretical control over the $1/k^2$ power term in the effective coupling and, thus, to reduce corresponding systematic error, might be not as hopeless a goal as it seems.

kinematical effects. 0.000; safe.

The structure of the PT spectrum is such that it respects the kinematical boundary $x \geq x_{\min} = 2M/W$ only in the first α_s order. Contribution to $\langle x_Q \rangle$ from potentially dangerous region between x_{\min} and $2x_{\min}$ can be estimated as

$$\Delta \langle x_Q \rangle \sim \alpha_s(W)/\pi \cdot (1 - \langle x_Q \rangle) \cdot x_{\min}^2,$$

which value is well below 1% even for x_{\min} as big as $1/3$.

¹²An older average $\langle x_{D^*} \rangle = 0.494 \pm 0.014$ which we have used in the previous analysis ^[32] was contaminated by the sea. We are indebted to P.Mättig for clarifying this point

quark masses. 0.002; conservative.

Given that the structure of low-momentum contribution proportional to \bar{A} naturally embodied into PT analysis reminds that of the shift from Euclidean to “on-shell” quark mass (see (4.7)), one may worry about *double counting* if the pole mass is used for M in the PT formulae. The problem should be studied theoretically. Meanwhile, let us mention that one may get equally good description of absolute values of mean quark energy losses with *smaller* (Euclidean?) quark masses plugged in. For example, by taking

$$M_c = 1.30 \text{ GeV}; \quad M_b = 4.50 \text{ GeV}$$

one obtains¹³

G_2 -model	C_2	χ^2	$\bar{A}(2\text{GeV})$	$\alpha_{\overline{\text{MS}}}(M_Z)$
$\Lambda^{(5)} = 600$	3.60	0.72	0.166	0.1280
$\Lambda^{(3+2)} = 740$	2.94	0.66	0.166	0.1257

We observe that the resulting value $\alpha_{\overline{\text{MS}}}(M_Z)$ hardly increases by 1 per mil.

Another feature of the alternative set of quark masses worth noticing is a systematic decrease of the value of characteristic integral \bar{A} . This may be a welcome trend bearing in mind a recent analysis of power corrections to jet shape variables, see [35]. For the time being we choose to look upon this 10% shift as a systematic uncertainty which will be greatly reduced when proper theoretical understanding of the nature of the quark mass parameter is achieved.

Having said that we modify (4.6b) and present the final result for the integrated coupling as

$$\bar{A}(2\text{GeV}) = 0.18 \pm 0.01 \text{ (stat)} \pm 0.02 \text{ (syst)}. \quad (4.11)$$

Finally, in Fig.13 we demonstrate the W -evolution of realistic c- and b-quark spectra obtained within the F -model with one-loop 3-flavour α_s^{eff} . These curves correspond to the values of A and Λ providing the best common fit to mean energy losses as described above. For comparison the best-fit G_2 -model curves are also shown for LEP energy. F - and G -model spectra are quite close to each other. We may conclude that it suffices to fix the integral parameter (4.6b) together with the value of Λ to predict the differential energy distributions with a reasonable accuracy¹⁴.

A stable numerical procedure for numerical evaluation of the inverse Mellin transform (2.4) remains to be designed.

5 Conclusions

Jets initiated by heavy quarks (b,c) are now extensively studied experimentally. The interest to this subject is connected not only with testing the fundamental aspects of QCD but also with its large potential importance for measurements of heavy particle properties: lifetimes, spatial oscillations of flavour, searching for CP violating effects in their decays *etc.* Properties

¹³4.5 is a preferable bottom mass value for $M_c=1.3$, analogously to $M_b=4.75$ for $M_c=1.5$; see above, Fig.8

¹⁴Let us notice that the differential quark energy spectra obtained by the inverse Mellin transform (2.4), (2.6) violate kinematical boundary $D(x < 2M/W) = 0$ at $\mathcal{O}(\alpha_s^2)$ level

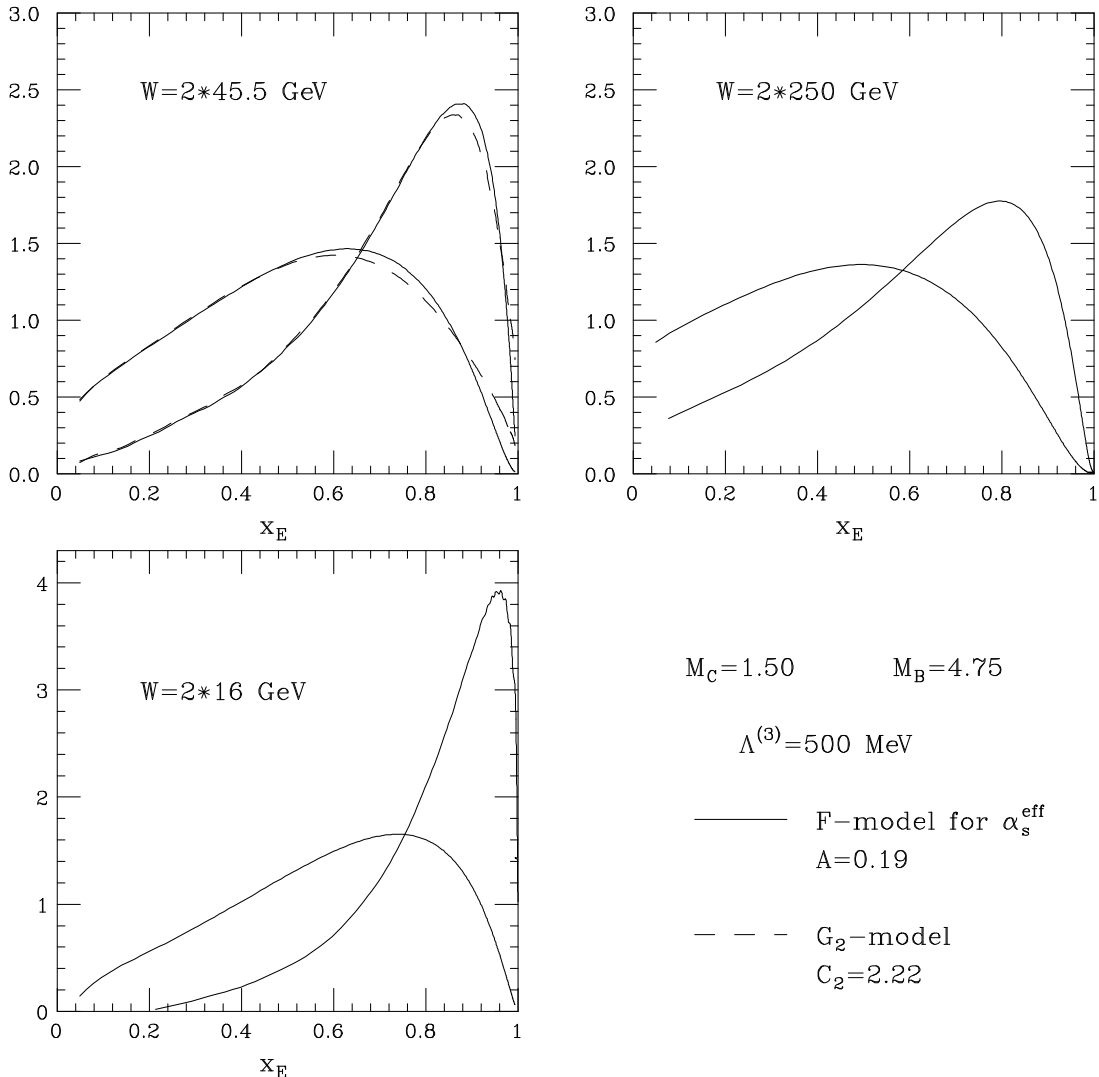


Figure 13: Evolution of inclusive c, b spectra from $W = 32\text{GeV}$ to $W = 500\text{GeV}$. The best-fit F -model (solid) and G_2 -model curves (dashed) are shown.

of b-initiated jets are of primary importance for analysis of the final state structure in the $t\bar{t}$ production processes.

In this paper we presented results of the study of the inclusive energy spectra of leading heavy-flavoured particles (H_Q) based on the perturbative expression (2.4) – (2.7) for heavy Q distributions that emerge after taking into proper account multiple gluon bremsstrahlung off the $Q\bar{Q}$ pair.

Our approximation includes the two-loop anomalous dimension, keeps track of the *collinear* logarithms $a \ln W$ and $a \ln M$, *soft* double-logarithmic $a \ln^2(1-x_Q)$ and essential single-logarithmic $a \ln(1-x_Q)$ contributions in all orders. At the same time, it embodies the exact first order result $\mathcal{O}(a)$ for the inclusive energy distribution which property is necessary to account for non-relativistic suppression of gluon radiation in the situation when jet energies are comparable with a heavy quark mass.

The spectra we have been considering correspond to *direct* Q production. Such an approach

disregards the sea contribution to heavy quark yield which is numerically small at present and foreseeable energies. Accordingly, a specific term in the non-singlet two-loop anomalous dimension has been omitted which is due to $Q\bar{Q}Q\bar{Q}$ final states and would violate the “multiplicity” sum rule (2.1).

Apart from this simplification, the formal relative accuracy of the perturbative result (2.4) – (2.7) is $\mathcal{O}(a^2(W^2))$ which estimate is *uniform* in x_Q . Perturbative corrections at the quark mass scale which were left out of control start from $\mathcal{O}(a^3(M^2))$.

We have formulated the perturbative result (2.4) – (2.7) in terms of a “physical” coupling, the one which directly measures radiation intensity of relatively soft gluons [22]. This coupling constant is different from (roughly, 10% larger than) $\alpha_{\overline{\text{MS}}}$ and is approximately related to the latter by (2.17b). Expressed in terms of α_s^{eff} , the radiator (2.7) acquires the two-loop contribution $\tilde{\Delta}^{(2)}$ which is free from an artificial n_f -dependence [23] and proves to be numerically negligible.

There are two ingredients of the standard approach to description of H_Q spectra. Here one starts from the phenomenological non-PT fragmentation function for the $Q \rightarrow H_Q$ transition and then traces its evolution with increase of the annihilation energy W by means of PT QCD. Being formally well justified for describing the W -evolution, this approach however leaves the dependence on the quark mass, M , basically out of the PT control.¹⁵

Motivated by the LPHD concept, we attempted to derive *pure* PT predictions without invoking the phenomenological fragmentation function. Starting point for such an attempt was the observation that an appearance of the parton model motivated *peak* in the non-PT fragmentation at large x_Q [27,9] can be attributed to the Sudakov suppression effects *provided* one feels courageous enough to continue the PT description down to the region of gluon transverse momenta, $k_\perp \sim \Lambda \cdot (W/\sqrt{M\Lambda})^{0.2}$, which at present (and foreseeable) energies looks dangerously close to the non-perturbative domain.

When getting rid of the transverse momentum cutoff one faces the problem of the formal “infrared pole” in α_s and is forced to introduce the effective non-singular coupling $\alpha_s^{\text{eff}}(k)$ that remains finite at $k \leq \Lambda$. It is not easy to justify the very notion of α_s at small momenta where the PT quark-gluon language seems to be hardly applicable at all. In the problem under consideration it can be related to the effective measure of intensity of accompanying particle production at the confinement stage of the H_Q formation, a finite number of light hadrons produced in addition to the (W dependent) particle yield due to PT-controlled gluon bremsstrahlung at the first stage of the hard $Q\bar{Q}$ pair creation process.

We have checked that, in accordance with expectations based on general factorization properties, our ignorance about confinement does not affect the W -dependence of the mean energy losses $\langle x_Q \rangle(W, M)$. Thus the ratio $\langle x_Q \rangle(W)/\langle x_Q \rangle(W_0)$ can be used to extract the fundamental QCD parameter Λ . Another infrared stable quantity found empirically is the PT prediction for the normalized peak position, $x_Q^{\text{peak}}(W)/x_Q^{\text{peak}}(W_0)$.

At the same time, the absolute values of $\langle x_Q \rangle$, peak positions and particle distributions in general show up substantial variations with the value (momentum dependence) of α_s^{eff} in the origin chosen as an input for calculating the PT *radiator* (2.7). We have compared experimental values of $\langle x_Q \rangle$ extracted from leptonic c- and b-quark decays and $\langle x_{D^*} \rangle$ directly with the PT

¹⁵A plausible rescaling procedure for extracting the non-PT part of the B meson fragmentation from the existing data on D meson spectra has been suggested recently in [11].

motivated prediction for the quark energy losses.

Our treatment of the hadronization stage that implicitly appeals to duality arguments makes it plausible to apply purely perturbative approach to inclusive quantities such as the lepton energy distributions. Meanwhile, it can not pretend to describe *exclusive* heavy hadron spectra such as those of D^* , for example. Therefore, taking the measured mean energies of D^* for $\langle x_Q \rangle$ might introduce some systematic uncertainty to the fit, the error which is difficult to estimate.

Nonetheless, such a comparison has demonstrated that radiative charm and beauty losses may be consistently described in the energy range $W = 10 \rightarrow 90 \text{ GeV}$ within a variety of models for low momentum behaviour of the infrared finite effective coupling α_s^{eff} . By tuning the shape parameter of a model one achieves an accuracy of the common fit as good as $\chi^2/\text{d.o.f.} \approx 0.7/5$ (7 data points; two free parameters, Λ and A/C).

We have checked that the fit to all data is consistent with the fits to high- W , D^* and inclusive lepton data samples.

From the first sight, we have gained not much profit since we had to pay for eliminating an arbitrary non-PT fragmentation function by introducing another arbitrary function $\alpha_s^{\text{eff}}(k)$ at $k \lesssim 2 \text{ GeV}$. An essential physically important difference between two approaches is that α_s^{eff} as a key ingredient of the PT-LPHD approach is supposed to be *universal* so that (quite substantial) differences between inclusive spectra of c- and b- flavoured hadrons should be under control. By simultaneous fitting of the available experimental data on the energy losses in charm and beauty sectors we have demonstrated consistency of the hypothesis of α_s^{eff} universality.

Moreover, the same notion of the infrared-finite effective coupling can be tried for a good many interesting problems in the light quark sector. An incomplete list of such phenomena for which the PT analysis has been carried out recently to next-to-leading order includes transverse ^[36] and longitudinal momentum distributions ^[37] in hadron-initiated processes, the energy-energy correlation ^[38], the thrust ^[39] and the heavy jet mass distribution ^[40] in e^+e^- annihilation.

The presence of the exponential of the characteristic integral over gluon momenta which emerges after all-order resummation of the Sudakov logarithms ^[41,42] is a common feature of the corresponding PT expressions. It is straightforward to derive quantitative PT-motivated predictions by implementing the universal α_s^{eff} in these integrals and, at the same time, by getting rid of non-PT “hadronization” effects which are usually taken into account by convoluting the PT distributions with phenomenological fragmentation functions (initial parton distributions for the case of hadron-initiated processes).

Carrying out this laborious but promising program one should get a valuable information about the confinement physics as seen through the eyes of the integrated influence of the large-distance hadron production upon inclusive particle distributions and/or event characteristics.

To this end the numerical results of our analysis of the heavy quark energy losses, namely,

$$(2\text{GeV})^{-1} \int_0^{2\text{GeV}} dk \frac{\alpha_s^{\text{eff}}(k)}{\pi} = 0.18 \pm 0.01 \text{ (exp)} \pm 0.02 \text{ (theor)} , \quad (5.1a)$$

$$\alpha_{\overline{\text{MS}}}^{\text{eff}}(M_Z) = 0.125 \pm 0.003 \text{ (exp)} \pm 0.004 \text{ (theor)} , \quad (5.1b)$$

should be looked upon as a first hint for the more detailed study including the light quark phenomena discussed above.

One comment is in order concerning the nature of the results (5.1). The parallel description of c,b losses is sensitive to α_s^{eff} in the low momentum range, say, of the order of (and below) M_b , so that the integral characteristic (5.1a) gets fixed quite sharply (theoretical error is due to our ignorance about the heavy quark masses and should be eliminated in the future).

At the same time such a description proves to be quite liberal to details of the high-momentum behaviour of the coupling (one- versus two-loop α_s , number of active quark flavours). From this point of view the value (5.1b) that one extracts in the end of the day is rather a tribute to (unfortunate) tradition. $\alpha_{\overline{\text{MS}}}^{\text{eff}}(M_Z)$ should be looked upon as a reference value which emerges after theoretical extrapolation rather than a quantity that is “measured” by the above analysis. Theoretical error in (5.1b) is dominated by potential k^{-2} power correction effects in $\alpha_s^{\text{eff}}(k)$.

Let us stress again that in the low momentum region behaviour of the effective coupling is poorly known not because of the limited knowledge of higher order effects but rather because of an essentially different physical phenomenon that enters the game, the one that is usually referred to as confinement.

From this point of view our notion of the infrared finite α_s^{eff} differs from one that emerges from the three-loop analysis based upon the renormalization-scheme-invariant approaches to the e^+e^- annihilation cross section [44,45] and the τ -lepton hadronic width [44]. Nevertheless it is worth mentioning that the value of the *couplant* $\frac{\alpha_s}{\pi}(0)$ and the integral measure obtained in [45] in the framework of the Minimal Sensitivity Principle [46] are consistent with (5.1a).

Phenomenological verification of the fact that the effective QCD coupling stays numerically small would be of large practical value. Gribov theory of confinement [29] demonstrates how colour confinement can be achieved in a field theory of light fermions interacting with comparatively small effective coupling — a fact of potentially great impact for enlarging the domain of applicability of perturbative ideology to the physics of hadrons and their interactions.

Acknowledgments

We are indebted to V.N. Gribov and P. Mättig for many helpful discussions and valuable comments. One of us (Y.D.) is most grateful to the Theory Department of the University of Lund for the warm hospitality extended to him during the years when this study was being performed. This work was supported in part by the UK Particle Physics and Astronomy Research Council.

Appendix A : Running coupling in the Radiator

A.1 Notation and Kinematics

We consider production of a $Q\bar{Q}$ pair with on-mass-shell 4-momenta p_1^μ , p_2^μ and a gluon with momentum k^μ by a colourless current with the total momentum q^μ . Hereafter for a sake of simplicity we measure all the momenta and the quark mass in units of the total annihilation energy ($q^2 \equiv W^2 = 1$).

In terms of quark and gluon energy fractions,

$$\begin{aligned} z_i &\equiv 2(p_i q), \quad z \equiv 2(kq); \quad z_1 + z_2 + z = 2; \\ 2p_1 p_2 &= (q - k)^2 - 2m^2 = 1 - z - 2m^2 + k^2 = z_1 + z_2 - 1 - 2m^2 + k^2; \end{aligned} \quad (\text{A.1})$$

virtual quark propagators are

$$\kappa_1 \equiv (p_1 + k)^2 - m^2 = 1 - z_2, \quad \kappa_2 \equiv (p_2 + k)^2 - m^2 = 1 - z_1. \quad (\text{A.2})$$

(Relations (A.2) do not imply $k^2 = 0$.)

Three-body kinematics restricts the difference of quark energy fractions as

$$4|\vec{k}|^2 \cdot \beta^2 \geq (z_1 - z_2)^2, \quad (\text{A.3a})$$

where $\beta = \beta(z)$ represents the quark velocity in the rest frame of the $Q\bar{Q}$ pair ($Q\bar{Q}$ cms):

$$\beta^2 \equiv \frac{p_{Q\bar{Q}}^2}{E_{Q\bar{Q}}^2} = 1 - \frac{4m^2}{(p_1 + p_2)^2} = 1 - \frac{4m^2}{(q - k)^2}. \quad (\text{A.3b})$$

A.1.1 $k^2 = 0$

For the on-mass-shell gluon case one has $4|\vec{k}|^2 = z^2$; $(q - k)^2 = 1 - z$ and (A.3) gives

$$\beta = \left(1 - \frac{4m^2}{1 - z}\right)^{\frac{1}{2}} \geq \left|\frac{z_1 - z_2}{z}\right|. \quad (\text{A.4})$$

z, Θ_c **Basis.** When the gluon energy is kept fixed, it is convenient to use the *scaled difference* of quark energies as a complementary variable related to the gluon angle in the $Q\bar{Q}$ cms:

$$u \equiv \frac{z_1 - z_2}{z} = \frac{2(p_1 - p_2)k}{2(p_1 + p_2)k} = \beta \cos \Theta_c; \quad -\beta \leq u \leq +\beta. \quad (\text{A.5})$$

The maximal value $|u| = \beta$ is reached when the gluon is *collinear* with one of the quarks.

Introducing maximal quark velocity v ,

$$\beta^2 \leq v^2 \equiv 1 - 4m^2 \geq z, \quad (\text{A.6})$$

one may present the integration phase space as

$$\int dz_1 \int dz_2 = \frac{1}{2} \int_0^{v^2} zdz \int_{-\beta}^{\beta} du. \quad (\text{A.7})$$

Useful relations:

$$1 - u^2 = 4(1 - z_1)(1 - z_2) \cdot z^{-2}; \quad (\text{A.8a})$$

$$\left(\frac{1-z_1}{1-z_2} + \frac{1-z_2}{1-z_1} \right) = \frac{z^2}{(1-z_1)(1-z_2)} - 2 = \frac{4}{1-u^2} - 2. \quad (\text{A.8b})$$

x, y Basis. For the purpose of deriving single-inclusive quark spectrum we break the symmetry between z_1, z_2 and denote

$$x \equiv z_1; \quad y \equiv 1 - z_2.$$

One has to fix x and integrate over y in the limits $y_- \leq y \leq y_+$ which follow from the kinematical restriction (A.4). In terms of x, y the latter takes the form

$$y^2(1 - x + m^2) - y(x - 2m^2)(1 - x) + m^2(1 - x)^2 \leq 0. \quad (\text{A.9})$$

This gives

$$y_{\pm} = \frac{1 - x}{2(1 - x + m^2)} (x - 2m^2 \pm \sqrt{x^2 - 4m^2}).$$

Introducing

$$z_0 \equiv \frac{1}{2} (x - 2m^2 + \sqrt{x^2 - 4m^2}) = x + \mathcal{O}(m^2), \quad (\text{A.10})$$

one may write (*cf.* (2.8))

$$\begin{aligned} y_+ &= \frac{(1 - x) z_0}{1 - x + m^2} = x \cdot (1 + \mathcal{O}(m^2)), \\ y_- &= \frac{1 - x}{z_0} m^2 = \frac{1 - x}{x} m^2 \cdot (1 + \mathcal{O}(m^2)). \end{aligned} \quad (\text{A.11})$$

Useful relations:

$$y_+ - y_- = \frac{1 - x}{1 - x + m^2} \sqrt{x^2 - 4m^2}, \quad (\text{A.12a})$$

$$(y_-)^{-1} - (y_+)^{-1} = \frac{\sqrt{x^2 - 4m^2}}{1 - x} m^{-2}, \quad (\text{A.12b})$$

$$(y_+)^2 - (y_-)^2 = (x - 2m^2) \sqrt{x^2 - 4m^2} \left(\frac{1 - x}{1 - x + m^2} \right)^2. \quad (\text{A.12c})$$

A.1.2 $k^2 > 0$

If we allow the gluon to have a positive virtuality k^2 , (A.3) takes the form

$$(z_1 - z_2)^2 \leq (z^2 - 4k^2) \left(1 - \frac{4m^2}{1 - z + k^2} \right) \quad (\text{A.13})$$

and leads to the following maximal invariant gluon mass for given z_1, z_2 :

$$\begin{aligned} k^2 \leq k_m^2 &= (1 - z_1)(1 - z_2) - \frac{1}{2} \left[z_1 z_2 - 4m^2 - \sqrt{z_1 - 4m^2} \sqrt{z_2 - 4m^2} \right] \\ &= \left\{ \frac{2(1 - x + m^2)}{x - (2 - x)y - 4m^2 + \sqrt{[x^2 - 4m^2][(1 - y)^2 - 4m^2]}} \right\} \cdot (y_+ - y)(y - y_-). \end{aligned} \quad (\text{A.14})$$

As we shall see below, the structure of the matrix element is such that essential contributions emerge from the logarithmic region $y_- \ll y \ll y_+$, as well as from the vicinity of the *lower* limit, $(y - y_-) \sim y_- \sim m^2$. Therefore for our purposes the following approximate expression suffices,

$$k_m^2 = (1 - x)(y - y_-) + \mathcal{O}(m^2), \quad (\text{A.15})$$

which differs from the exact formula (A.14) only in a tiny region close to the *upper* integration limit, $(y_+ - y) \sim m^2$.

Two characteristic momentum scales emerge related to the limiting values of the y -integration (*cf.* (2.8))

$$\begin{aligned} \mathcal{Q}^2(x) &\equiv W^2 \cdot (1 - x)y_+ \approx W^2 x(1 - x); \\ \kappa^2(x) &\equiv W^2 \cdot (1 - x)y_- \approx M^2(1 - x)^2/x. \end{aligned} \quad (\text{A.16})$$

A.2 VASP Cross Sections

The differential first order cross section integrated over angles of the final $Q\bar{Q}g$ system may be written as

$$\left\{ \frac{d^2\sigma_{Q\bar{Q}g}}{dz_1 dz_2} \right\}_C = \sigma^\infty \cdot \frac{C_F \alpha_s}{2\pi} \Pi_C. \quad (\text{A.17})$$

The subscript C marks the production current (vector (V), axial vector (A), scalar (S) or pseudoscalar (P)) and σ^∞ is the universal high-energy limit of the Born transition probability, Current(C) $\rightarrow Q\bar{Q}$.

Straightforward calculation leads to the following expression for the Π factors¹⁶:

$$\Pi_C = 2\zeta_C \mathcal{S} + \mathcal{H}_C; \quad (\text{A.18a})$$

$$\mathcal{H}_V = \left(\frac{1 - z_1}{1 - z_2} + \frac{1 - z_2}{1 - z_1} \right) = (1 - x) \cdot \frac{1}{y} + \frac{y}{1 - x}, \quad (\text{A.18b})$$

$$\mathcal{H}_A = (1 + 2m^2)\mathcal{H}_V + 4m^2, \quad \mathcal{H}_S = \mathcal{H}_P = \mathcal{H}_V + 2. \quad (\text{A.18c})$$

¹⁶see [25] for details

Here \mathcal{S} is the “soft” bremsstrahlung term

$$\begin{aligned}\mathcal{S} \equiv -\left(\frac{p_{1\mu}}{\kappa_1} - \frac{p_{2\mu}}{\kappa_2}\right)^2 &= \frac{z_1 + z_2 - 1 - 2m^2}{(1-z_1)(1-z_2)} - \frac{m^2}{(1-z_1)^2} - \frac{m^2}{(1-z_2)^2} \\ &= \frac{x-2m^2}{1-x} \cdot \frac{1}{y} - \frac{m^2}{y^2} - \frac{1-x+m^2}{(1-x)^2}.\end{aligned}\quad (\text{A.19})$$

Its contribution to each of the squared matrix elements is explicitly proportional to corresponding ζ -factor, the one that determines energy dependence of the corresponding $Q\bar{Q}$ Born cross section,

$$\sigma_{Q\bar{Q}} = \sigma^\infty \cdot v \zeta_C(v); \quad (\text{A.20a})$$

$$\begin{aligned}\zeta_V &= \frac{3-v^2}{2} = 1+2m^2, \\ \zeta_A &= \zeta_S = v^2 = 1-4m^2, \quad \zeta_P = 1.\end{aligned}\quad (\text{A.20b})$$

As a result, the *normalized* differential distribution can be written in the following general form as a sum of a *universal* “ \mathcal{S} ” and a process dependent “ \mathcal{H} ” contribution:

$$d^2w_C \equiv \left\{ \frac{d^2\sigma_{Q\bar{Q}g}}{\sigma_{Q\bar{Q}}} \right\}_C = \frac{C_F\alpha_s}{2\pi v} \left\{ 2\mathcal{S} + \zeta_C^{-1} \mathcal{H}_C \right\} dx dy. \quad (\text{A.21})$$

z, Θ_c **Basis.** Both structure of the matrix element and kinematics become particularly simple in terms of the gluon energy fraction and the gluon angle in the $Q\bar{Q}$ cms (see (A.5)). Making use of (A.8) one gets

$$\mathcal{S} = \frac{4(1-z)}{z^2} \frac{\beta^2 - u^2}{(1-u^2)^2} = \frac{4(1-z)}{z^2} \frac{\beta^2 \sin^2 \Theta_c}{(1-\beta^2 \cos^2 \Theta_c)^2} \frac{4m^2}{1-z+4m^2}; \quad (\text{A.22a})$$

$$\mathcal{H}_V = \frac{4}{1-u^2} - 2 = \frac{4}{1-\beta^2 \cos^2 \Theta_c} - 2. \quad (\text{A.22b})$$

Invoking (A.7), (A.21) we obtain for the inclusive gluon energy spectrum in the vector channel (see also [26])

$$dw_V = \frac{C_F\alpha_s}{\pi} \frac{dz}{z} \frac{\beta}{v} \int_{-1}^1 d\cos \Theta_c \left\{ 2(1-z) \frac{\beta^2 \sin^2 \Theta_c}{(1-\beta^2 \cos^2 \Theta_c)^2} + z^2 \left[\frac{1}{1-\beta^2 \cos^2 \Theta_c} - \frac{1}{2} \right] \zeta_V^{-1} \right\}. \quad (\text{A.23})$$

Our convention to call the two pieces of the matrix element “soft” and “hard” becomes clear now: in the soft gluon limit, $z \ll 1$, the second term is z^2 down compared to the first one. In this representation the “dead cone” phenomenon is also manifesting: the soft *classical* term \mathcal{S} vanishes in the very forward directions ($\Theta_c, \pi - \Theta_c < \theta_0 = m$).

In relativistic situation ($m \ll \frac{1}{2}$) a collinear logarithmic enhancement occurs and the two pieces of (A.23) participate in forming the GLAP splitting function,

$$dw \propto \frac{d\Theta_c^2}{\Theta_c^2} \left\{ 2(1-z) + z^2 \right\} \frac{dz}{z} \propto \frac{1+(1-z)^2}{z} dz.$$

It is worthwhile to notice that $\mathcal{O}(z^{-1})$ and $\mathcal{O}(1)$ parts of the $q \rightarrow q + g(z)$ splitting function are process independent, while the $\mathcal{O}(z)$ piece breaks factorization at the level of $\mathcal{O}(m^2 \ln m^2)$ correction. Therefore the very notion of “fragmentation function” as a way of treating the jet evolution independently of the production mechanism gets lost beyond leading twist.

To stress logarithmic character of the angular integration one may represent (A.23) as

$$dw_V = \frac{C_F \alpha_s}{\pi v} \frac{dz}{z} \int_{\eta_0}^1 \frac{d\eta}{\sqrt{1-\eta}} \left\{ 2(1-z) \frac{\eta - \eta_0}{\eta^2} + z^2 \left[\frac{1}{\eta} - \frac{1}{2} \right] \zeta_V^{-1} \right\}, \quad (\text{A.24a})$$

where

$$\eta \equiv 1 - u^2 = 1 - \beta^2 \cos^2 \Theta_c \geq \eta_0 \equiv \frac{4m^2}{1-z}. \quad (\text{A.24b})$$

For other production channels the second “hard” term in (A.23), (A.24a) should be changed according to (A.18c), (A.20b).

A.3 Integration over Virtual Boson Mass

Considering *inclusive* characteristics (*e.g.*, such as the quark energy spectrum) beyond the first order of perturbation theory one has to allow the gluon to decay in the final state, that is to have a positive virtuality k^2 , and to integrate over the latter within the available phase space. Actually, only such a combination of real and virtual gluon production leads to a sensible physical answer. First of all, an *exclusive* real gluon production cross section is clearly zero because of the standard infinite (double logarithmic) Sudakov form factor suppression. Secondly, and more importantly, a “real” gluon is an ill-defined object since its “on-mass-shell” interaction strength α_0 may not be defined perturbatively (which is a real “infrared catastrophe” inherent for QCD).

Integration over k^2 leads to appearance of the running coupling in the inclusive cross section. This nice property discovered in the pioneering papers by Gribov and Lipatov on partonic structure of logarithmic field theories [18] is particularly helpful in the QCD context. Here neither α_0 in “elastic” radiation nor small virtuality inelastic gluon decay systems are well defined. Meanwhile, their combined action results in a legitimate $\alpha_s(k_m)$ at the Euclidean scale related to the maximal available gluon virtuality.

We shall demonstrate this correspondence taking care of subleading effects which might be relevant within the adopted approximation. To this end we write down a formal dispersion relation (with one subtraction) for the running coupling

$$\alpha(Q^2) \equiv \alpha_0 \cdot \mathcal{Z}_3(-Q^2) = \alpha_0 + Q^2 \int_0^\infty \frac{dk^2}{k^2} \frac{\sigma(k^2)}{k^2 + Q^2}, \quad (\text{A.25a})$$

where σ is related to discontinuity of \mathcal{Z}_3 at positive virtuality,

$$\sigma(k^2) \equiv \frac{\alpha_0}{2\pi i} \left[\mathcal{Z}_3(k^2 - i\epsilon) - \mathcal{Z}_3(k^2 + i\epsilon) \right] \equiv -\frac{\alpha_0}{2\pi} \text{Disc} \left\{ \mathcal{Z}_3(k^2) \right\}. \quad (\text{A.25b})$$

In QED \mathcal{Z}_3 is nothing but the photon renormalization function and $\alpha_0 \approx 1/137$ — the on-mass-shell coupling constant.

Strictly speaking, such an identification is true for an Abelian theory only. In the QCD context the Ward identity between vertex and fermion propagator corrections, $\mathcal{Z}_\Gamma \mathcal{Z}_q = 1$, does not hold. As well known, both the non-Abelian vertex renormalization correction $\mathcal{Z}_\Gamma^{(\text{na})}$ and the gluon propagator factor \mathcal{Z}_g participate (in a gauge dependent way) in forming the running α_s . So one has to look upon \mathcal{Z}_3 in the dispersion relation (A.25) as the gauge invariant product

$$\mathcal{Z}_3 = \mathcal{Z}_\Gamma^{(\text{na})} \cdot \mathcal{Z}_g \cdot \mathcal{Z}_\Gamma^{(\text{na})}.$$

This subtlety does not affect the result, however.

Another motivation is to use the n_f dependence as a gauge to pinpoint the structure of the running α_s in the inclusive cross section [23]. Quark loops (in order α^2) belong to \mathcal{Z}_g only, and employing a “quasi-Abelian” relation (A.25) becomes natural.

In the problem under consideration the following structure emerges,

$$\begin{aligned} & \alpha_0 M(z_1, z_2; 0) + \int_0^{k_m^2} \frac{dk^2}{k^2} \sigma(k^2) \cdot M(z_1, z_2; k^2) \\ &= \left\{ \alpha_0 + \int_0^{k_m^2} \frac{dk^2}{k^2} \sigma(k^2) \right\} M(z_1, z_2; 0) + \int_0^{k_m^2} dk^2 \sigma(k^2) \cdot \Delta M(z_1, z_2; k^2), \end{aligned} \quad (\text{A.26})$$

with $k_m^2 = k_m^2(z_1, z_2)$ the maximal squared virtual boson mass allowed for given x, y . Here we have singled out the $k^2 = 0$ part of the matrix element by writing

$$M(z_1, z_2; k^2) = M(z_1, z_2; 0) + k^2 \cdot \Delta M(z_1, z_2; k^2). \quad (\text{A.27})$$

Now we may relate the characteristic integral in the first term in the rhs of (A.26) with the dispersion formula (A.25a). To this end we employ the following *exact* representation of the dispersion relation

$$\alpha(Q^2) = \alpha_0 + Q^2 \int_0^\infty \frac{dk^2 \sigma(k^2)}{k^2(k^2 + Q^2)} = \alpha_0 + \int_0^{Q^2} \frac{dk^2}{k^2} \sigma(k^2) + \int_0^1 \frac{dt}{1+t} \left[\sigma(Q^2/t) - \sigma(Q^2 t) \right]. \quad (\text{A.28})$$

Perturbatively, σ is of the order of α^2 . As a result, the last finite integral term constitutes a *next-to-next-to-leading* correction to the main one. To see this one has to view σ as a slowly varying (logarithmic) function of its argument¹⁷ and to perform the Taylor expansion in $\ln Q^2$ to obtain

$$\int_0^1 \frac{dt}{1+t} \left[\sigma(Q^2/t) - \sigma(Q^2 t) \right] = -2\sigma'(Q^2) \int_0^1 \frac{dt}{1+t} \ln t + \mathcal{O}(\sigma''') \approx \frac{\pi^2}{6} \sigma'(Q^2).$$

This exercise demonstrates a close correspondence between the spectral density (A.25b) and the β -function [47]:

$$\alpha(Q^2) = \alpha_0 + \int_0^{Q^2} \frac{dk^2}{k^2} \sigma(k^2) + \frac{\pi^2}{6} \sigma'(Q^2) + \dots; \quad (\text{A.29a})$$

$$\sigma(Q^2) = \alpha'(Q^2) - \frac{\pi^2}{6} \alpha'''(Q^2) + \mathcal{O}(\alpha^{(V)}). \quad (\text{A.29b})$$

¹⁷which is true everywhere except in the very vicinity of a fermion threshold

Thus we express perturbatively the structure in curly brackets of (A.26) in terms of the running coupling at the Euclidean point $Q^2 = k_m^2$:

$$\tilde{\alpha}(k_m^2) \equiv \left\{ \alpha_0 + \int_0^{k_m^2} \frac{dk^2}{k^2} \sigma(k^2) \right\} = \alpha(k_m^2) - \frac{\pi^2}{6} \alpha''(k_m^2) + \dots \quad (\text{A.30})$$

A.4 Running Coupling in the First Order Spectrum

It is straightforward to calculate the exact $Q\bar{Q}g$ matrix element with account of a non-zero virtual gluon mass $k^2 > 0$. (A.21) gets modified as follows:

$$2\mathcal{S} \implies 2\mathcal{S}^{(0)} - k^2 \left(\frac{1}{(1-z_1)^2} + \frac{1}{(1-z_2)^2} \right); \quad (\text{A.31a})$$

$$\mathcal{H}_V \implies \mathcal{H}_V^{(0)} + 2k^2 \frac{z_1 + z_2 + k^2}{(1-z_1)(1-z_2)}, \quad (\text{A.31b})$$

where $\mathcal{S}^{(0)}$ and $\mathcal{H}_V^{(0)}$ are given by the original ‘‘on-mass-shell-boson’’ expressions (A.19) and (A.18b) respectively. In terms of (A.27),

$$\Delta \{ 2\mathcal{S} \} = -\frac{1}{y^2} - \frac{1}{(1-x)^2}; \quad (\text{A.32a})$$

$$\Delta \{ \mathcal{H}_V \} = \frac{2(1+x-y+k^2)}{(1-x)y}. \quad (\text{A.32b})$$

A.4.1 $k^2 = 0$ part of the matrix element.

To evaluate the radiator (2.7) we start by considering the first term in (A.26) proportional to $M(z_1, z_2; 0)$. One has to perform the y -integral with the factor $\tilde{\alpha}$ that emerges after integration over virtual boson mass, see (A.30),

$$\int_{y_-}^{y_+} dy \tilde{\alpha}(k_m^2(x, y)) \cdot \left\{ 2\mathcal{S}^{(0)} + \zeta_V^{-1} \mathcal{H}^{(0)} \right\}, \quad (\text{A.33})$$

with k_m^2 given by the approximate expression (A.15). Invoking (A.19), (A.18b) we split the integrand into three pieces as follows:

$$\left\{ 2\mathcal{S}^{(0)} + \zeta_V^{-1} \mathcal{H}^{(0)} \right\} = \left\{ 2 \frac{x-2m^2}{1-x} + \zeta_V^{-1}(1-x) \right\} \frac{1}{y} \quad (\text{A.34a})$$

$$- 2 \frac{m^2}{y^2} \quad (\text{A.34b})$$

$$- 2 \frac{1-x+m^2}{(1-x)^2} + \zeta_V^{-1} \frac{y}{1-x}. \quad (\text{A.34c})$$

Logarithmic Piece (A.34a). This is the leading contribution to the radiator, in which the y -integration is logarithmic (collinear log):

$$\int_{y_-}^{y_+} \frac{dy}{y} \tilde{\alpha}(y - y_-) . \quad (\text{A.35})$$

Here we have explicitly shown the essential y -dependence of the coupling factor $\tilde{\alpha}$. The chain of approximations follows:

$$\begin{aligned} (\text{A.35}) &= \int_{y_-}^{y_+} \frac{dy}{y} \left(\tilde{\alpha}(y) + \tilde{\alpha}'(y) \ln \frac{y - y_-}{y} + \dots \right) \approx \int_{y_-}^{y_+} \frac{dy}{y} \tilde{\alpha}(y) + \tilde{\alpha}'(y) \int_{\frac{y_-}{y_+}}^1 \frac{ds}{s} \ln(1 - s) \\ &\approx \int_{y_-}^{y_+} \frac{dy}{y} \tilde{\alpha}(y) - \frac{\pi^2}{6} \tilde{\alpha}'(y_-) = \int_{\kappa^2}^{Q^2} \frac{dt}{t} \alpha(t) - \frac{\pi^2}{6} \alpha'(\kappa^2) + \mathcal{O}(\alpha^3(\kappa^2) + \alpha^3(Q^2)) , \end{aligned} \quad (\text{A.36})$$

where (A.30) has been used. We notice that a potential second order contribution $\alpha' \propto \alpha^2$ at the *low* scale $\kappa^2 \sim M^2$ cancels out, and the remaining term $\alpha'(\kappa^2) \propto \alpha^2(W^2)$ is comparable with the two-loop correction to the *hard cross section* (coefficient function) and must be neglected within our approximation.

Finally,

$$\int dy (\text{A.34a}) = \left(2 \frac{x - 2m^2}{1 - x} + \zeta_V^{-1}(1 - x) \right) \int_{\kappa^2}^{Q^2} \frac{dt}{t} \alpha(t) . \quad (\text{A.37})$$

Singular Piece (A.34b). The second term of (A.34) originates from the dead cone subtraction. It is explicitly proportional to m^2 but this suppression gets compensated by the singular behaviour in y . Corresponding y -integral is concentrated in a tiny region $(y - y_-) \sim y_- \propto m^2$:

$$\int_{y_-}^{y_+} \frac{dy}{y^2} \tilde{\alpha}(y - y_-) = \alpha(y_-) \int_{y_-}^{y_+} \frac{dy}{y^2} + \alpha'(y_-) \int_{y_-}^{y_+} \frac{dy}{y^2} \ln \frac{y - y_-}{y_-} + \mathcal{O}(\alpha''(y_-)) \quad (\text{A.38})$$

The $\mathcal{O}(\alpha^2(y_-))$ term vanishes in the relativistic approximation:

$$\int_{y_-}^{y_+} \frac{dy}{y^2} \ln \frac{y - y_-}{y_-} = \int_0^{\frac{y_+ - y_-}{y_-}} \frac{ds}{(1 + s)^2} \ln s \approx \int_0^\infty \frac{ds}{(1 + s)^2} \ln s = 0 .$$

Thus, similarly to what has happened to the logarithmic term (A.34a) discussed above, a potential $\mathcal{O}(\alpha^2(\kappa))$ contribution is absent. One is left with a pure $\alpha(\kappa^2)$ correction to the radiator:

$$\int dy (\text{A.34b}) = -2m^2 \left\{ \frac{1}{y_-} - \frac{1}{y_+} \right\} \alpha(\kappa^2) = -2 \frac{\sqrt{x^2 - 4m^2}}{1 - x} \alpha(\kappa^2) . \quad (\text{A.39})$$

Finite Piece (A.34c). Corresponding y -integral is collinear safe (*i.e.* finite in the $m^2 = 0$ limit) and constitutes $\alpha(W^2)$ correction to the hard cross section. Here one extracts the coupling at

the upper limit, $y \sim y_+$, and the y -integration becomes trivial (see (A.12)):

$$\begin{aligned} \int dy \ (A.34c) &= \alpha(Q^2) \left\{ -2 \frac{(1-x+m^2)(y_+ - y_-)}{(1-x)^2} + \zeta_V^{-1} \frac{\frac{1}{2}(y_+^2 - y_-^2)}{1-x} \right\} \left[1 + \mathcal{O}(\alpha(Q^2)) \right] \\ &\approx \alpha(Q^2) \sqrt{x^2 - 4m^2} \left\{ -\frac{2}{1-x} + \zeta_V^{-1} \frac{x-2m^2}{2(1-x)} \left(\frac{1-x}{1-x+m^2} \right)^2 \right\}. \end{aligned} \quad (\text{A.40})$$

A.4.2 Δ part of the matrix element.

From the first sight, corrections (A.32) to the $Q\bar{Q}g$ matrix element proportional to virtual boson mass look negligible: corresponding k^2 integration is no longer logarithmic, $k^2 \sim k_m^2$, and the result is of the order of $\sigma(k_m^2) \propto \alpha^2(k_m^2)$.

This expectation indeed comes true for the “hard” correction term (A.32b) as well as for the second piece of (A.32a). However, the first contribution to the “soft” correction term (A.32a) is *over-singular* in y , as a result of which singularity logarithmic behaviour gets restored and a contribution to the two-loop anomalous dimension emerges.

Indeed,

$$\int_0^{k_m^2} dk^2 \sigma(k^2) = k_m^2 \left\{ \sigma(k_m^2) + \sigma'(k_m^2) \int_0^{k_m^2} \frac{dk^2}{k_m^2} \ln \frac{k^2}{k_m^2} + \dots \right\} \equiv k_m^2 \cdot \tilde{\sigma}(k_m^2), \quad (\text{A.41a})$$

where

$$\tilde{\sigma} = \alpha' - \alpha'' + \mathcal{O}(\alpha'''). \quad (\text{A.41b})$$

Invoking (A.15) for k_m^2 one arrives at the following expression for the Δ -correction:

$$- (1-x) \int_{y_-}^{y_+} \frac{dy}{y^2} (y - y_-) \cdot \tilde{\sigma}(y - y_-) \quad (\text{A.42})$$

An approximate evaluation follows:

$$\begin{aligned} \int_{y_-}^{y_+} \frac{dy}{y^2} (y - y_-) \tilde{\sigma}(y - y_-) &= \int_{y_-}^{y_+} \frac{dy}{y^2} (y - y_-) \tilde{\sigma}(y) + \mathcal{O}(\tilde{\sigma}'(y_-)) \\ &\approx \int_{y_-}^{y_+} \frac{dy}{y} \tilde{\sigma}(y) - \tilde{\sigma}(y_-) = \left[\alpha(Q^2) - \alpha(\kappa^2) - \alpha'(Q^2) + \alpha'(\kappa^2) \right] - \left[\alpha'(\kappa^2) + \dots \right]. \end{aligned} \quad (\text{A.43})$$

Again, as before, the $\alpha^2(\kappa^2)$ contribution cancels, and one finally gets the correction

$$\int dy \int dk^2 \sigma(k^2) \Delta M(x, y; k^2) = -(1-x) \left[\alpha(Q^2) - \alpha(\kappa^2) \right] + \mathcal{O}(\alpha^2(Q^2) + \alpha^3(\kappa^2)). \quad (\text{A.44})$$

Combining (A.37), (A.39), (A.40) and (A.44) we finally arrive at the expression (2.7) for the perturbative radiator.

Appendix B : Second loop Anomalous Dimension $\Delta^{(2)}$

B.1 AD (dimensional regularization)

The two-loop anomalous dimension (AD) has been derived in the framework of dimensional regularization approach in [19–21]. In notations of Curci, Furmanski and Petronzio [19] the non-singlet AD corresponding to $Q \rightarrow Q$ transition in *space-like* evolution reads (eqs. (4.50) – (4.54) of [19])

$$C_F^{-1} \hat{P}_{qq}(x, a) = aP(x) + a^2 \gamma^{(2)}(x), \quad P(x) \equiv \frac{1+x^2}{1-x};$$

$$\gamma^{(2)} = C_F P_F(x) + C_A P_G(x) + n_f T_R P_{n_f}(x),$$
(B.1)

where

$$P_F = -2P(x) \ln x \ln(1-x) - \left(\frac{3}{1-x} + 2x \right) \ln x - \frac{1}{2}(1+x) \ln^2 x - 5(1-x) \quad (B.2a)$$

$$P_G = P(x) \left[\frac{1}{2} \ln^2 x + \frac{11}{6} \ln x + \frac{67}{18} - \frac{\pi^2}{6} \right] + (1+x) \ln x + \frac{20}{3}(1-x) \quad (B.2b)$$

$$P_{n_f} = -\frac{2}{3} \left[P(x) \left(\ln x + \frac{5}{3} \right) + 2(1-x) \right]. \quad (B.2c)$$

Let us mention an extra contribution due to $Q \rightarrow \bar{Q} + QQ$ transition which reads

$$C_F^{-1} \hat{P}_{q\bar{q}}(x, a) = a^2 \left(C_F - \frac{1}{2} C_A \right) \{ 2P(-x) S_2(x) + 2(1+x) \ln x + 4(1-x) \}, \quad (B.3a)$$

with

$$S_2(x) \equiv \int_{x(1+x)^{-1}}^{(1+x)^{-1}} \frac{dz}{z} \ln \frac{1-z}{z}. \quad (B.3b)$$

This contribution (which formally belongs to the *non-singlet* AD, see, *e.g.*, [15]) vanishes as $(1-x)^2$ at large x , is colour suppressed and numerically negligible. In this paper it has been disregarded together with the *singlet* (sea) contribution to heavy quark yield.

An algebraic massage leads to the following representation for the quark evolution kernel¹⁸:

$$C_F^{-1} \hat{P}_{qq}(x, a) = [a + \mathcal{K}a^2] P(x) + a^2 \{ \sigma \cdot C_F \mathcal{V}(x) + \mathcal{R}(x) \} - a' [P(x) \ln x + 2(1-x)]. \quad (B.4)$$

The first term here collects the one-loop AD with the part of $\gamma^{(2)}$ correction explicitly proportional to $P(x)$ with the number \mathcal{K} given by (2.16b) above. These two combine forming a “physical” coupling in terms of the $\overline{\text{MS}}$ one according to (2.17b). This term totally absorbs the $(1-x)^{-1}$ singularity of the evolution kernel: $\mathcal{V}(x) \propto \ln(1-x)$ and $\mathcal{R}(x)$ vanishes as $(1-x)$ in the quasi-elastic limit.

¹⁸The “+” prescription is implicit.

(The very last term in (B.4) proportional to the derivative of the running coupling,

$$a' \equiv \frac{d}{d \ln W^2} \frac{\alpha_s(Q)}{2\pi} = - \left(\frac{11}{6} N_c - \frac{2}{3} T_R n_f \right) a^2 + \dots, \quad (\text{B.5})$$

does not count, as it is an artefact of the dimensional regularization scheme; see below.)

The “true” second loop AD in curly brackets of (B.4) consists of two contributions. The first one is

$$\begin{aligned} \mathcal{V}(x) &= - \left[P(x) \left(\ln \frac{x}{(1-x)^2} - \frac{3}{2} \right) + (1-x) - \frac{1}{2}(1+x) \ln x \right] \ln x \\ &= \int_0^1 dz \int_0^1 dy \delta(x-yz) \{P(y)\}_+ P(z) \ln z. \end{aligned} \quad (\text{B.6a})$$

So defined, \mathcal{V} has a very simple form in the moment representation, namely,

$$\mathcal{V}(j) \equiv \int_0^1 dx x^{j-1} \mathcal{V}(x) = P_j \frac{d}{dj} P_j. \quad \left(P_j \equiv \int_0^1 dx P(x)_+ = \int_0^1 dx [x^{j-1} - 1] \frac{1+x^2}{1-x} \right) \quad (\text{B.6b})$$

(Obviously, $[\mathcal{V}(x)]_+ = \mathcal{V}(x)$.) This (and only this) contribution changes (acquires an opposite sign) when time-like evolution is considered [19]. Therefore (B.4) holds for both channels with $\sigma = \pm 1$ referring to time- and space-like evolution correspondingly. The origin of the \mathcal{V} term in the two-loop kernel may be traced back to a simple kinematical difference between annihilation and scattering channels [19]. It has been argued [48] that a mismatch between the two-loop e^+e^- and DIS anomalous dimensions would disappear (and thus the Gribov-Lipatov relation [18] would be rescued) if one considered scaling violation of “pseudo-moments” in x evaluated for a fixed value of $\{xW^2\}_{\text{annih.}} = \{Q^2/x\}_{\text{scatt.}}$.

Another term of the second loop AD is

$$\mathcal{R}(x) = \left(\frac{1}{2} C_A - C_F \right) P(x) \ln^2 x - 5C_F \left[\frac{1}{2}(1+x) \ln x + (1-x) \right] + C_A \left[(1+x) \ln x + 3(1-x) \right]. \quad (\text{B.7})$$

Similarly to the one-loop splitting function $P(x)$, it obeys the reciprocity relation [18]

$$-x\mathcal{R}(x^{-1}) = \mathcal{R}(x), \quad (\text{B.8a})$$

and, as a result, stays the same for time- and space-like evolution. Contrary to this,

$$-x\mathcal{V}(x^{-1}) = [-1] \cdot \mathcal{V}(x). \quad (\text{B.8b})$$

B.2 CF (dimensional regularization)

$\mathcal{O}(a)$ correction to the hard cross section [19,20] (coefficient function; CF) has to be taken into consideration together with the two-loop AD since neither CF nor AD is a scheme independent quantity beyond leading logs.

It reads (see eqs. (7.4), (7.10) of [19])

$$\begin{aligned} C_2^A &= \delta(1-x) + aC_F \left\{ \left[\frac{1+x^2}{1-x} \left(\ln \frac{1-x}{x} - \frac{3}{4} \right) + \frac{1}{4}(9+5x) \right]_+ \right. \\ &\quad \left. + \frac{3(1+x)^2}{1-x} \ln x - \frac{7}{2}(1+x) + \pi^2 \delta(1-x) \right\}; \end{aligned} \quad (\text{B.9a})$$

$$C_L^A = aC_F. \quad (\text{B.9b})$$

The first line of (B.9a) is the CF for the scattering channel (C_2^S); the second line accounts for their difference. After simple manipulations one arrives at

$$C_2^A = (1 - \frac{3}{2}aC_F)\delta(1-x) + aC_F \left[P(x) \left(\ln[x^2(1-x)] - \frac{3}{4} \right) - \frac{1}{4}(5+9x) \right]_+. \quad (\text{B.10})$$

In the cross section integrated over total $Q\bar{Q}g$ production angle (see (2.3)) the combination $C_2^A + 3C_L^A$ emerges. With account of the longitudinal contribution the $\delta(1-x)$ -term gets modified,

$$\begin{aligned} C^A(x, a) \equiv C_2^A + 3C_L^A &= (1 - \frac{3}{2}aC_F)\delta(1-x) + aC_F[(\text{B.10})]_+ + 3aC_F \\ &= (1 + \frac{3}{2}aC_F)\delta(1-x) + aC_F[(\text{B.10}) + 3]_+. \end{aligned} \quad (\text{B.11})$$

Constructing the CF that describes quark distribution *normalized* by the total cross section,

$$C_t(x, a) = (1 + \frac{3}{2}aC_F)^{-1} \cdot C^A(x, a), \quad (\text{B.12})$$

one gets, with $\mathcal{O}(a)$ accuracy, the answer which may be presented in the following form:

$$\begin{aligned} C_t(x, a) &= \delta(1-x) + aC_F \left[P(x) \left(\ln[x(1-x)] - \frac{3}{4} \right) - \frac{1}{4}(1+x) \right]_+ \\ &\quad + aC_F \{ P(x) \ln x + 2(1-x) \}_+. \end{aligned} \quad (\text{B.13})$$

B.3 Scaling Violation Rate

Scaling violation rate is an observable determined by the scheme invariant combination

$$D' \equiv \frac{d}{d \ln W^2} D(x, W^2) \implies \hat{P}_{qq}(x, a(W^2)) + \frac{d}{d \ln W^2} C_t(x, a(W^2)). \quad (\text{B.14})$$

Combining (B.4) and (B.13) one arrives at ¹⁹

$$\begin{aligned} D' \implies & \left[a_{\overline{\text{MS}}} + \mathcal{K}a^2 \right] C_F P(x) + a^2 C_F \{ C_F \mathcal{V}(x) + \mathcal{R}(x) \} \\ & + a' C_F \left[P(x) \left(\ln[x(1-x)] - \frac{3}{4} \right) - \frac{1}{4}(1+x) \right], \end{aligned} \quad (\text{B.15})$$

where the $\overline{\text{MS}}$ origin of the running coupling has been stressed in the relevant first order term.

¹⁹The “+” prescription is implicit.

This result has to be compared with the scaling violation rate as described by (2.7). To this end one evaluates the $\ln W^2$ derivative of the relativistic radiator (2.10) to obtain

$$D' \implies \left\{ a(\mathcal{Q}^2) C_F P(x) - a' C_F (1-x) + a^2 C_F \Delta^{(2)} \right\} + a' C_F \left\{ \frac{-2x}{1-x} + \frac{x^2}{2(1-x)} \right\}. \quad (\text{B.16})$$

In the leading term one has to expand the coupling of a composite argument \mathcal{Q}^2 near W^2 as follows,

$$a(\mathcal{Q}^2) = a(W^2) + a' \ln[x(1-x)] + \dots \quad (\text{B.17})$$

Adding together terms proportional to a' one observes correspondence with a relevant part of (B.15):

$$\begin{aligned} -\frac{2x}{1-x} &= -P(x) + (1-x), & \frac{x^2}{2(1-x)} &= \frac{1}{4}P(x) - \frac{1}{4}(1+x); \\ \ln[x(1-x)] - (1-x) - \frac{2x}{1-x} + \frac{x^2}{2(1-x)} &= P(x) \left(\ln[x(1-x)] - \frac{3}{4} \right) - \frac{1}{4}(1+x). \end{aligned}$$

Identifying

$$(B.15) = (B.16) \quad (\text{B.18})$$

we arrive at the final result which relates an “effective” (dispersion scheme motivated) coupling a_{eff} with $a_{\overline{\text{MS}}}$ and gives an expression for the “true” second loop correction to the radiator $\tilde{\Delta}^{(2)}$ we were aiming at:

$$a_{\text{eff}} C_F P(x) + a^2 C_F \tilde{\Delta}^{(2)} = \left[a_{\overline{\text{MS}}} + \mathcal{K}a^2 \right] C_F P(x) + a^2 C_F \{ C_F \mathcal{V}(x) + \mathcal{R}(x) \}. \quad (\text{B.19})$$

References

- [1] for reviews see, *e.g.*,
P. Mättig, Talk at the 4th Int. Symp. on Heavy Flavour Physics; Bonn preprint, Bonn-HE-91-19 (1991);
T. Behnke in: Proc. of the 26th Int. Conf. on High Energy Physics, Dallas, Texas, 1992, ed. J.R Sanford, AIP Conference Proceedings, vol. I, p.859;
see also T. Behnke to be published in: Proc. of the Conf. QCD-94, Montpellier, France, 1994;
P.S. Wells, preprint CERN-PPE/94-203 (1994).
- [2] for recent publications see, *e.g.*,
OPAL Collaboration, R. Akers *et al.*, *Zeit.Phys.* **C60** (1993) 199 ;
SLD Collaboration, K. Abe *et al.*, *Phys.Rev.Lett.* **72** (1994) 3145 ;
OPAL Collaboration, R. Akers *et al.*, *Zeit.Phys.* **C61** (1994) 209 ;
A.De Angelis *et al.*, DELPHI Report, DELPHI 94-94, PHYS 411 ;
ALEPH Collaboration, D. Buskulic *et al.*, *Zeit.Phys.* **C62** (1994) 1, *ibid.* **C62** (1994) 179.
- [3] Yu.L. Dokshitzer, V.S. Fadin and V.A. Khoze, *Phys.Lett.* **115B** (1982) 242;
Zeit.Phys. **C15** (1982) 325.
- [4] Yu.L. Dokshitzer, V.A. Khoze and S.I. Troyan, in: Proc. of the 6th Int. Conf. on Physics in Collisions, p.417, ed. M. Derrick, World Scientific, Singapore, 1987.
- [5] Yu.L. Dokshitzer, Light and Heavy Quark Jets in Perturbative QCD, in: *Physics up to 200 TeV*, Proc. of the Int. School of Subnuclear Physics, Erice, 1990, vol.28, Plenum Press, New York, 1991.
- [6] Yu.L. Dokshitzer, V.A. Khoze, S.I.Troyan, *J.Phys.G: Nucl.Part.Phys.* **17**(1991) 1481, 1602.
- [7] Yu.L. Dokshitzer, V.A. Khoze, S.I.Troyan, “Specific Features of Heavy Quark Production. I. Leading quarks”, Lund preprint LU TP 92-10;
Yu.L. Dokshitzer, in: *Perturbative QCD and Hadronic Interactions*, Proc. of the 27th Rencontres de Moriond, p.259, ed. J.Tran Thanh Van, Editions Frontières, Gif-sur-Yvette, 1992.
- [8] V.A. Khoze, in: Proc. of the 26th Int. Conf. on High Energy Physics, Dallas, Texas, 1992, ed. J.R. Sanford, AIP Conference Proceedings, vol. II, p. 1578; Durham preprint DTP/93/78.
- [9] C. Peterson *et al.*, *Phys.Rev.* **D27** (1983) 105; for review see, *e.g.*,
M. Bosman *et al.*, Heavy Flavours, in: Proc. of the Workshop on Z physics at LEP, CERN Report 89-08, ed. G. Altarelli, R. Kleiss and C. Verzegnassi, volume 1, p.267, 1989;
J.H. Kühn and P.M. Zerwas, in Advanced Series in Directions in High Energy Physics, “Heavy Flavours”, ed. A.J. Buras and M. Lindner, World Scientific, Singapore 1992, p. 434.

- [10] B. Mele and P. Nason, *Phys.Lett.* **245B** (1990) 635; *Nucl.Phys.* **B361** (1991) 626.
- [11] G. Colangelo and P. Nason, *Phys.Lett.* **285B** (1992) 167.
- [12] Yu.L. Dokshitzer, V.A. Khoze, A.H. Mueller and S.I. Troyan, *Basics of Perturbative QCD*, ed. J.Tran Thanh Van, Editions Frontières, Gif-sur-Yvette, 1991.
- [13] V.N. Baier and V.A. Khoze, *Sov.Phys.JETP* **21** (1965) 629; preprint NSU, Novosibirsk, 1964.
- [14] V.S. Fadin and V.A. Khoze, *JETP Lett.* **46** (1987) 525; *Sov.J.Nucl.Phys.* **48** (1988) 309.
- [15] G. Altarelli, *Phys.Rep.* **81** (1982) 1.
- [16] Yu.L. Dokshitzer, D.V. Shirkov, “On Exact Account of Heavy Quark Thresholds in Hard Processes”, Lund preprint LU TP 93-19; unpublished.
- [17] L. Trentadue, in: *Perturbative QCD and Hadronic Interactions*, Proc. of the 27th Rencontres de Moriond, p.167, ed. J.Tran Thanh Van, Editions Frontières, Gif-sur-Yvette, 1992.
- [18] V.N. Gribov and L.N. Lipatov, *Sov.J.Nucl.Phys.* **15** (1972) 438, 675.
- [19] G. Curci, W. Furmanski and R. Petronzio, *Nucl.Phys.* **B175** (1980) 27.
- [20] G. Altarelli, R.K. Ellis, G. Martinelli and S.Y. Pi, *Nucl.Phys.* **B160** (1979) 301.
- [21] W. Furmanski and R. Petronzio, *Phys.Lett.* **97B** (1980) 437, *Zeit.Phys.* **C11** (1982) 293; J. Kalinowski, K. Konishi, P.N. Scharbach and T.R. Taylor, *Nucl.Phys.* **B181** (1981) 253; E.G. Floratos, C. Kounnas and R. Lacaze, *Nucl.Phys.* **B192** (1981) 417.
- [22] S. Catani, G. Marchesini and B.R. Webber, *Nucl.Phys.* **B349** (1991) 635.
- [23] S.J. Brodsky, G.P. Lepage and P.R. MacKenzie, *Phys.Rev.* **D28** (1983) 228; for a recent review see S.J. Brodsky and H.J. Lu, SLAC-PUB-6683 (1994).
- [24] F.E. Low, *Phys.Rev.* **D110** (1958) 974 ;
T.H. Burnett and N.M. Kroll, *Phys.Rev.Lett.* **20** (1968) 86.
- [25] Yu.L. Dokshitzer, V.A. Khoze and W.J. Stirling, *Nucl.Phys.* **B428** (1994) 3.
- [26] V.N. Baier, V.S. Fadin and V.A. Khoze, *Nucl.Phys.* **B65** (1973) 381.
- [27] Ya.I. Azimov, L.L. Frankfurt, V.A. Khoze, Preprint LNPI-222, 1976; in: *Proc. of the XVIII Int. Conf. on High Energy Physics, Tbilisi, 1976*, Dubna, II:B10, 1977; J. Bjorken, *Phys.Rev.* **D17** (1978) 171; M. Suzuki, *Phys.Lett.* **71B** (1977) 139.
- [28] R.L. Jaffe and L. Randall, *Nucl.Phys.* **B412** (1994) 79.

- [29] V.N. Gribov, Possible Solution of the Problem of Quark Confinement, LU TP 91-7, 1991.
- [30] I.I. Bigi, M.A. Shifman, N.G. Uraltsev and A.I. Vainshtein, *Phys.Rev.* **D50** (1994) 2234; M. Beneke and V.M. Braun, *Nucl.Phys.* **B426** (1994) 301.
- [31] M.B. Voloshin and Yu.M. Zaitsev, *Sov.Phys.Usp.* **30** (1987) 553.
- [32] Yu.L. Dokshitzer, V.A. Khoze, S.I. Troyan, “Specific Features of Heavy Quark Production. II. LPHD Approach to Heavy Particle Spectra”, Lund preprint LU TP 94-23.
- [33] M.H. Seymour, *Zeit.Phys.* **C63** (1994) 99.
- [34] OPAL Collaboration, R.Akers et al., CERN-PPE/94-217, CERN-PPE/95-058.
- [35] Yu.L. Dokshitzer and B.R. Webber, *Phys.Lett.* **352B** (1995) 451.
- [36] J. Kodaira and L. Trentadue, *Phys.Lett.* **112B** (1982) 66; C.T.H. Davies, J. Stirling and B.R. Webber, *Nucl.Phys.* **B256** (1985) 413; J.C. Collins, D.E. Soper and G. Sterman, *Nucl.Phys.* **B250** (1985) 199; S. Catani, E. d’Emilio and L. Trentadue, *Phys.Lett.* **211B** (1988) 335.
- [37] G. Sterman, *Nucl.Phys.* **B281** (1987) 310; S. Catani and L. Trentadue, *Phys.Lett.* **217B** (1989) 539; *Nucl.Phys.* **B327** (1989) 323; *Nucl.Phys.* **B353** (1991) 183.
- [38] J. Kodaira and L. Trentadue, *Phys.Lett.* **123B** (1982) 335; preprint SLAC-PUB-2934 (1982).
- [39] S. Catani, G. Turnock, B.R. Webber and L. Trentadue, *Phys.Lett.* **263B** (1991) 491.
- [40] S. Catani, G. Turnock and B.R. Webber, *Phys.Lett.* **272B** (1991) 368.
- [41] Yu.L. Dokshitzer, D.I. Dyakonov and S.I. Troyan, *Phys.Lett.* **84B** (1979) 234; *Phys.Rep.* **C58** (1980) 270; A. Bassutto, M. Ciafaloni and G. Marchesini, *Nucl.Phys.* **B163** (1980) 477; G. Curci and M. Greco, *Phys.Lett.* **92B** (1980) 175.
- [42] G. Parisi and R. Petronzio, *Nucl.Phys.* **B154** (1979) 427; B.R. Webber and P. Rakow, *Nucl.Phys.* **B187** (1981) 254.
- [43] Yu.L. Dokshitzer, V.A. Khoze and S.I. Troyan, *Zeit.Phys.* **C55** (1992) 107.
- [44] J. Chyla, A. Kataev, S.A. Larin, *Phys.Lett.* **267B** (1991) 269.
- [45] A.C. Mattingly and P.M. Stevenson, *Phys.Rev.Lett.* **69** (1992) 1320.
- [46] P.M. Stevenson, *Phys.Rev.* **D23** (1981) 2916.
- [47] J. Schwinger, *Proc.Nat.Acad.Sci.USA* **71** (1974) 5047.
- [48] Yu.L. Dokshitzer, Talk given at the HERA Workshop, DESY, September 1993, unpublished.